LUT University

Intricate features of electron and hole skew scattering in semiconductors

Rakitskii M. A., Denisov K. S., Lähderanta E., Rozhansky I. V.

This is a Author's accepted manuscript (AAM) version of a publication

published by American Physical Society

in Physical Review B

DOI: 10.1103/PhysRevB.106.085203

Copyright of the original publication:

©2022 American Physical Society

Please cite the publication as follows:

Rakitskii, M. A., Denisov, K. S., Lähderanta, E., Rozhansky, I. V. (2022). Intricate features of electron and hole skew scattering in semiconductors. Physical Review B, vol. 106, iss. 8. DOI: 10.1103/PhysRevB.106.085203

This is a parallel published version of an original publication. This version can differ from the original published article.

Intricate features of electron and hole skew scattering in semiconductors

M. A. Rakitskii,[1] K. S. Denisov,[1] E. Lähderanta,[1] and I. V. Rozhansky[1,2,*]

[1] *LUT University, FI-53851 Lappeenranta, Finland*

[2] *Department of Condensed Matter Physics, Weizmann Institute of Science, Rehovot, 76100, Israel*

(Dated: February 8, 2023)

We study features of mobile carriers' skew scattering in nonmagnetic semiconductors emerging due to a combination of spin-orbit coupling in a crystal band structure and a nontrivial inner structure of impurities. In particular, we show that a nonzero magnetic moment of the impurity generally leads to the anomalous Hall effect (AHE) in the absence of the spin polarization of the mobile carriers, the effect arising from spin-independent scattering asymmetry due to exchange interaction. We analyze the skew scattering in bulk zinc-blende semiconductors for both electron and hole states and emphasize the crucial role of the impurity spin polarization for the emergent AHE for the valence band holes. We also revisit the skew scattering in quantum wells showing that the cancellation of the extrinsic contribution to the AHE common for two-dimensional systems can be lifted off depending on both the electron wave function and the impurity structure.

I. INTRODUCTION

A variety of spin transport phenomena constituting the core of modern spintronics are based on the spin separation, and, more generally, charge carriers' separation by their spin, valley, or pseudospin characteristic [1, 2]. The transverse spin separation is important for the spin-orbit torques [3, 4] and also can be combined with spin to charge conversion [5]. Naturally, the comprehensive understanding of microscopics underlying these phenomena is essential for the progress in the domain.

Skew scattering of electrons on electrically charged dopants has been long known as an extrinsic mechanism of the spin Hall effect (SHE) and anomalous Hall effect (AHE) [6, 7]. It is generally accepted that it stems from the spin-orbit coupling (SOC) as described by Mott and further developed by Smith [8, 9]. In the course of time it has been established that this effect is sensitive both to the microscopic mechanism of the SOC and also to the inner structure of the scatterer. For instance, in the original viewpoint of Mott scattering it is assumed that the SOC is provided by the core electric fields generated by a heavy impurity atom. It has been also shown that the role of the impurity-driven SOC can be to introduce the fine structure of the virtual bound states, i.e., the energy splittings with respect to the total angular momentum [10, 11]. Consequently, the resonant scattering on the virtual bound states leads to the enhancement of the anomalous Hall effect [11, 12].

Apart from the atomic structure of the charged scattering center itself, the extrinsic mechanism of the AHE can be induced by the complex structure of the electronic band states originating from the SOC in the host material [13]. When SOC affects the crystal band structure, the electron scattering on a spin-independent potential such as a Coulomb center becomes asymmetrical [14, 15]. In this case the Hall response depends on the host material properties; calculations of the Hall resistivity lead to qualitatively different results strongly depending on the model of the crystal SOC. For instance, for a 2D case the skew scattering can be suppressed for the Rashba model [16, 17], but not for Dirac electrons [13, 18].

The physical picture of the skew scattering and AHE becomes more complicated when both an impurity has a complex inner structure and the electronic band structure is modified by SOC. To date this situation has been mostly considered for metallic systems via first-principles calculations [19–22]. A particularly interesting situation occurs when the impurity has an inner magnetic moment. The break of time-reversal symmetry required for the skew scattering can then be provided by the scatterer magnetic moment rather than by incident electron spin polarization; consequently, the AHE can emerge even for nonpolarized electrons [11, 23–25].

While some discussion is going on for metallic systems [19–21], the effects of the interplay between impurity inner moment and SOC-affected band structure on the anomalous transport in semiconductors are much less investigated. In semiconductors the features of the skew scattering can be analyzed analytically in the vicinity of the Brillouin zone center (Γ point). That makes it possible to clarify the physics responsible for the modification of AHE. For metallic systems an accurate analysis of the skew scattering requires more detailed description of the band structure thus requiring DFT-based numerical approaches [19–21].

In the present paper we consider various cases of skew scattering of electrons and holes resulting from the combination of the SOC in the host nonmagnetic crystal and an inner magnetic moment of an impurity. On the basis of k.p theory for an electronic band structure we derive analytical results for the skew scattering rates and the associated AHE conductivity covering both bulk and two-dimensional types of spectrum. We demonstrate that the properties of skew-scattering induced AHE and SHE are essentially sensitive to microscopic details of the con-

* rozhansky@gmail.com

sidered material systems, as well as to the features of the impurities providing richer access to the microscopic physics of the effect.

The crystal band structure accounted for in our considerations also gives rise to intrinsic mechanisms of AHE and SHE [7, 18], so it is worth commenting on conditions when the considered extrinsic contribution would play the dominant role in experiments. The skew scattering appears in the first order with respect to the scattering time $\sigma_H \propto \tau$, while other mechanisms of AHE, including Berry's phase, side jump, or cluster skew scattering [26], behave as $\sigma_H \propto \tau^0$ leading to different scaling laws between transversal and longitudinal resistivities for the skew scattering $\rho_H \propto \rho_{xx}$ and $\rho_H \propto \rho_{xx}^2$ for all others. Therefore, the analysis presented in this paper is valid for sufficiently clean samples [27] ($\rho_{xx}^2 \ll \rho_{xx}$) with some fraction of impurities having finite magnetic moment. One example of a nonmagnetic semiconductor where the AHE is argued to be driven by carrier skew scattering on magnetic dopants is high-mobility electron gas in ZnO-based structures [23]. Also, we focus on essentially nonmagnetic semiconductors when the small density of magnetic impurities does not lead to the spontaneous spin splitting of the band states. In this sense we expect the Berry's phase dissipationless contribution to AHE [28] to be entirely suppressed.

Various intrinsic mechanisms underlying SHE and AHE in semiconductors have been discussed for the valence band holes [28–33]. The skew scattering of the holes in III-V semiconductors in the context of the extrinsic AHE has been believed to be similar to that of the electrons. Moreover, the effect is expected to be stronger as there is no small parameter Δ/E_0 (where Δ is the spin-orbit splitting and E_0 is the band gap) controlling SOC for the conduction band electrons. However, in a dilute p-type (Ga,Mn)As magnetic semiconductor for low resistivities the transverse vs longitudinal resistance scaling is quadratic or at least considerably superlinear suggesting that the dominating mechanism of AHE can be other than the skew scattering [34–36]. In metals such scaling can be also explained by inelastic scattering of electrons on phonons and spin waves [6]. Essentially, the domination of superlinear scaling mechanisms is favored for a larger resistance assuming the system is still beyond hopping conductivity [37]. Moreover, the microscopic mechanism of the valence band holes' skew scattering in semiconductors and its difference from the electron skew scattering has not been investigated theoretically. Neither has skew scattering of holes on magnetic centers been studied so far.

The paper is organized as follows. In Sec. II we present the model framework for analysis of asymmetric scattering contribution to the AHE. In the following sections the approach is applied to the relevant cases.

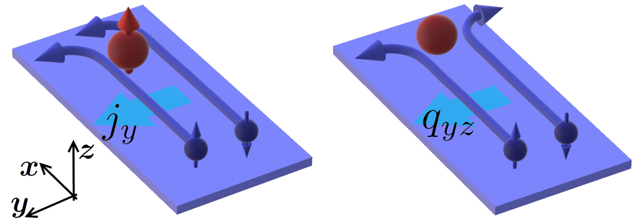

(a) Charge Hall effect. (b) Spin Hall effect.

FIG. 1: Illustration of spin-independent (a) and spin-dependent (b) contributions to the skew scattering leading, respectively, to charge Hall effect and spin Hall effect.

II. GENERAL THEORY

We analyze skew-scattering driven contributions to the transverse electric and spin Hall currents on the basis of the Boltzmann kinetic equation:

$$(e\boldsymbol{E}\boldsymbol{v}_s)\frac{\partial f_s^0}{\partial \varepsilon} = \mathrm{St}[\delta f_s], \tag{1}$$

where $f_s = f_s^0 + \delta f_s$ is the carrier distribution function (index s accounts for the spin states), which consists of the equilibrium f_s^0 and non-equilibrium δf_s parts, $\boldsymbol{E}$ is an applied electric field, $\boldsymbol{v}_s = \partial\varepsilon_s/\partial\boldsymbol{p}$ is a velocity in s-subband. The collision integral can be written as

$$\mathrm{St}[\delta f_s(\boldsymbol{k})] = \tag{2}$$
$$= \frac{2\pi}{\hbar} n_i \sum_{\boldsymbol{k}' s'} \delta(\varepsilon_k^s - \varepsilon_{k'}^{s'}) \left(|T_{kk'}^{ss'}|^2 \delta f_{s'}(\boldsymbol{k'}) - |T_{k'k}^{s's}|^2 \delta f_s(\boldsymbol{k}) \right),$$

where n_i is the impurity concentration, $\varepsilon_{\boldsymbol{k}}^s$ is a particle energy in s-subband and $T_{kk'}^{ss'}$ is the corresponding scattering T-matrix element for the scattering from the state $(\boldsymbol{k}, s)$ into the state $(\boldsymbol{k'}, s')$.

The skew-scattering contributions are related to the asymmetric parts of $|T_{kk'}^{ss'}|^2$. In this paper we treat the electron scattering on an impurity characterized by a potential $\hat{V}$ perturbatively. The corresponding T-matrix can be expanded in Born series

$$\hat{T} = \hat{V} + \hat{V}\hat{G}_0\hat{V} + \dots, \tag{3}$$

where $\hat{G}_0$ is the free Greens's function of mobile carriers in a semiconductor. As it is well known, the skew scattering does not appear in the first Born approximation so one should keep the second order in (3). The asymmetric term $W_{kk'}^{ss'}$ in $|T_{kk'}^{ss'}|^2$ takes the form [18]

$$W_{kk'}^{ss'} = 2\pi \sum_l \nu_l(\varepsilon) \langle \mathrm{Im}(V_{k'k}^{s's} V_{kq}^{sl} V_{qk'}^{ls'}) \rangle_{\Omega_q}, \tag{4}$$

where the sum is over the spin of the intermediate state, ν_l is the density of states (DOS) in l-subband, and $<>_{\Omega_q}$

denotes averaging over the angles of the intermidiate state wavevector $\boldsymbol{q}$. Note that in some cases the third order contribution to $W_{kk'}^{ss'}$ might vanish, so one should go in higher orders of the Born series [17, 38]. In this paper we deal with systems where the third-order contribution plays the major role. In the following sections we analyze the features of $W_{kk'}^{ss'}$ for different cases and describe the related properties of the emerging Hall response.

We assume relaxation time approximation and split the collision integral into two parts:

$$\begin{aligned}
&\mathrm{St}[\delta f_s(\boldsymbol{k})] = \mathrm{St}_1[\delta f_s(\boldsymbol{k})] + \mathrm{St}_2[\delta f_s(\boldsymbol{k})] \\
&\mathrm{St}_1[\delta f_s(\boldsymbol{k})] = \frac{2\pi}{\hbar} n_i \sum_{s',\boldsymbol{k'}} \delta(\varepsilon_k^s - \varepsilon_{k'}^{s'}) |V_{kk'}^{ss'}|^2 \delta f_{s'}(\boldsymbol{k'}) - \frac{\delta f_s(\boldsymbol{k})}{\tau_s}, \\
&\mathrm{St}_2[\delta f_s(\boldsymbol{k})] = \frac{2\pi}{\hbar} n_i \sum_{s',\boldsymbol{k'}} \delta(\varepsilon_k^s - \varepsilon_{k'}^{s'}) W_{kk'}^{ss'} \delta f_{s'}(\boldsymbol{k'}),
\end{aligned} \tag{5}$$

where τ_s is the quantum scattering time:

$$\frac{1}{\tau_s} = \frac{2\pi}{\hbar} n_i \sum_{s',\boldsymbol{k'}} \delta(\varepsilon_k^s - \varepsilon_{k'}^{s'}) |V_{k'k}^{s's}|^2. \tag{6}$$

The first part St_1 of the collision integral is of the second order in $\hat{V}$ and determines the longitudinal current. The second part St_2 is of the third order, it describes the scattering asymmetry leading to the transverse current. With the non-equilibrium part of the distribution function obtained from the kinetic equation the charge and currents are given by

$$\boldsymbol{j} = e \sum_{s,\boldsymbol{k}} \boldsymbol{v}_s f_s(\boldsymbol{k}). \tag{7}$$

In a 3D case it is convenient to expand the non-equilibrium part of the distribution function in the first spherical harmonics Y_x, Y_y and Y_z.

$$\delta f_s(\boldsymbol{k}) = f_x^s(k) Y_x + f_y^s(k) Y_y + f_z^s(k) Y_z, \tag{8}$$

$$Y_x = \sqrt{\frac{3}{4\pi}} \sin\theta\cos\varphi \;\; Y_y = \sqrt{\frac{3}{4\pi}} \sin\theta\sin\varphi \;\; Y_z = \sqrt{\frac{3}{4\pi}} \cos\theta.$$

Higher harmonics appear to give no contribution to the transverse current. Let the external electric field $\boldsymbol{E}$ be aligned along the x axis. As it will be shown below $W_{kk'}$ and $|V_{kk'}|^2$ can be represented in the following form:

$$\begin{aligned}
&W_{kk'}^{ss'} = w_{ss'}(Y_x' Y_y - Y_y' Y_x), \\
&|V_{kk'}^{ss'}|^2 = const + u_{ss'}(Y_x Y_x' + Y_y Y_y' + Y_z Y_z').
\end{aligned} \tag{9}$$

where a prime symbol denotes the spherical harmonic function dependence on (φ', θ') and rather than on (φ, θ).

In 2D case these formulas keep the same form with angular harmonics being $Y_x = \pi^{-1/2}\cos\varphi$, $Y_y = \pi^{-1/2}\sin\varphi$, $Y_z = 0$. Then the kinetic equation (1) can be rewritten in the matrix form (see appendix for details)

$$eE_x \frac{\partial f^0}{\partial \varepsilon} \begin{pmatrix} V \\ 0 \end{pmatrix} = \begin{pmatrix} A & -B \\ B & A \end{pmatrix} \begin{pmatrix} F_x \\ F_y \end{pmatrix}, \tag{10}$$

where V is a vector composed of the velocities in each spin subband, F_x and F_y are vectors containing the unknown coefficients for the expansion of the nonequilibrium part of the distribution function in angular harmonics, A and B are $n_s \times n_s$ matrices originating from the first and second parts of the collision integral, respectively (here, n_s is the number of spin subbands and ν' is the DOS in s'-subband):

$$\begin{aligned}
&V = \begin{pmatrix} v_1 \\ \vdots \\ v_{n_s} \end{pmatrix} \quad F_x = \begin{pmatrix} f_x^1 \\ \vdots \\ f_x^{n_s} \end{pmatrix} \quad F_y = \begin{pmatrix} f_y^1 \\ \vdots \\ f_y^{n_s} \end{pmatrix} \\
&A_{ss'} = \nu' u^{ss'} - \delta_{ss'} {\tau_s}^{-1} \qquad B_{ss'} = \nu' w^{ss'}
\end{aligned} \tag{11}$$

Neglecting the second part of the collision integral (of the higher order in V), we find the coefficients f_x^s.

$$F_x = eE_x \frac{\partial f^0}{\partial \varepsilon} A^{-1} V. \tag{12}$$

The longitudinal conductivity is further calculated according to:

$$j_x = e \sum_{s,\boldsymbol{k}} v_x^s \delta f_s. \tag{13}$$

Then, using the second part of the collision integral, the coefficients f_y^s are expressed in terms of the obtained coefficients f_x^s:

$$F_y = -A^{-1} B F_x = -eE_x \frac{\partial f^0}{\partial \varepsilon} A^{-1} B A^{-1} V. \tag{14}$$

At zero temperatures one has $(f^0)' = -\delta(\varepsilon - \varepsilon_F)$ and the transverse charge current can be calculated from

$$\begin{aligned}
&j_y = e \sum_s \int \nu_s \langle v_y^s \delta f^s \rangle_\Omega d\varepsilon = \\
&e \sum_s \int \nu_s v_s f_y^s d\varepsilon = e^2 E_x \sum_s \nu_s v_s (A^{-1} B A^{-1} V)_s.
\end{aligned} \tag{15}$$

One should note that the presence of asymmetric scattering does not guarantee the emergence of a charge Hall current. Firstly, the contributions to $W_{kk'}^{ss'}$ from different spin subbands can compensate each other when substituted into collision integral so that all the coefficients f_y^s will be equal to zero. Secondly, even for nonzero f_y^s, cancelling can occur when the transverse current is summed over different subbands with a non-zero current in each.

III. BULK ZINC-BLENDE SEMICONDUCTORS

In this section we consider skew-scattering of the mobile carriers for bulk semiconductors with zinc-blende crystal structure. Throughout our calculations we use the 14-band $\boldsymbol{k.p}$ model for GaAs-like semiconductors as shown in Fig. 2. For the electrons the $\boldsymbol{k.p}$ coupling between Γ_6^c conductance band and $\Gamma_{7,8}^v$ valence band is essential to capture the appearance of the skew-scattering. However, as it will be shown below this coupling remains crucial for the skew scattering of the valence band holes, as well as the coupling with p-like states corresponding to high-lying conduction bands $\Gamma_{7,8}^c$.

We model the scattering potential of an impurity with the following expression

$$\hat{V} = u(\boldsymbol{r}) + \hat{u}_X(\boldsymbol{r})\boldsymbol{J}\cdot\hat{\boldsymbol{\sigma}}, \tag{16}$$

where the first scalar term describes the electrostatic potential of an impurity and the second term $\hat{u}_X$ represents exchange interaction of itinerant electrons and localized spin $\boldsymbol{J}$ of the impurity. The electron spin is described by the Pauli matrices operator. In this work we treat the impurity spin $\boldsymbol{J}$ as a fixed vector and do not account for its dynamics (though some interesting effects can arise in the Kondo regime [22]). Let us assume that a weak external magnetic field is applied to a sample to maintain impurity magnetization $\boldsymbol{J} = J\boldsymbol{e}_z$.

The T-matrix includes matrix elements of both scalar and exchange parts of the scattering potential. We keep to a short-range impurity potential and describe its scalar part by a single matrix element u_0 unique for all Bloch states:

$$u_0 = \langle S|u|S\rangle = \langle X|u|X\rangle = \langle X'|u|X'\rangle, \tag{17}$$

where S, (X,Y,Z), (X',Y',Z') denote the Bloch amplitudes of the conductance band Γ_6^c, valence band $\Gamma_{7,8}^v$ and upper conductance band $\Gamma_{7,8}^c$, respectively. The matrix elements of the exchange interaction part calculated for different Bloch amplitudes are taken different:

$$\alpha_{ex} = \langle S|u_X|S\rangle,\ \beta_{ex} = \langle X|u_X|X\rangle,\ \gamma_{ex} = \langle X'|u_X|X'\rangle, \tag{18}$$

the off-diagonal matrix elements are assumed to be zero [39].

A. Conduction band Γ_6^c

Let us describe the skew-scattering of electrons in the conduction band Γ_6^c. The main effect leading to a finite skew-scattering comes from the inner spin-orbit coupling responsible for the valence band splitting Δ into Γ_7^v and Γ_8^v states [40] (see Fig. 2). The electron wave-function with account for the admixtrure of spin-orbit split valence band has the following form [14, 41]:

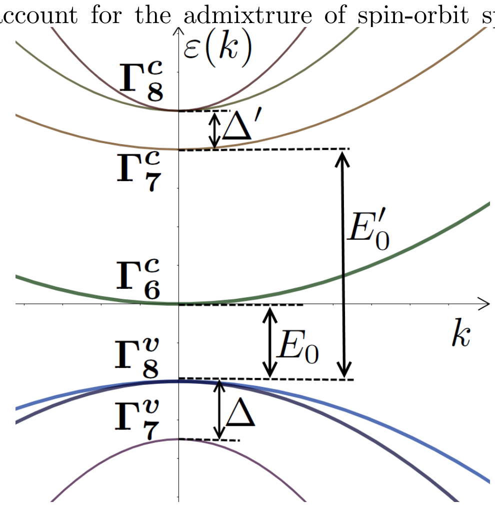

FIG. 2: Band diagram for a semiconductor with zinc-blend crystal structure.

$$\Psi_{\boldsymbol{k},s} = e^{i\boldsymbol{kr}}\Big(S + i\boldsymbol{R}\big(\mathcal{A}\boldsymbol{k} - i\mathcal{B}(\hat{\boldsymbol{\sigma}}\times\boldsymbol{k})\big)\Big)|\chi_s\rangle, \tag{19}$$

$$\mathcal{A} = P\frac{3E_0 + 2\Delta}{3E_0(E_0+\Delta)}, \quad \mathcal{B} = -P\frac{\Delta}{3E_0(E_0+\Delta)}, \tag{20}$$

$$P = \frac{i\hbar}{m}\langle S|\hat{p}_x|X\rangle, \tag{21}$$

where S is the Bloch amplitudes for the conduction band Γ_6^c and $\boldsymbol{R} = (X,Y,Z)$ are the degenerate valence band states at Γ point in the absence of spin-orbit splitting Γ_{15}, $|\chi_s\rangle = |\uparrow,\downarrow\rangle$ denotes the electron spin. The parameter $\mathcal{B}$ appears only due to nonzero Δ; this term is vital for the appearance of the scattering asymmetry.

The matrix element of the scattering potential given by Eq. 16 calculated between $\Psi_{\boldsymbol{k},s}$ and $\Psi_{\boldsymbol{k}',s'}$ states is given by

$$\begin{aligned}\hat{V}_{kk'} =& u_0\left(1 + (\mathcal{A}^2 + 2\mathcal{B}^2)(\boldsymbol{k}\cdot\boldsymbol{k}') + i(2\mathcal{A}\mathcal{B} + \mathcal{B}^2)\hat{\boldsymbol{\sigma}}\cdot(\boldsymbol{k}\times\boldsymbol{k}')\right) + \alpha_{ex}(\boldsymbol{J}\cdot\hat{\boldsymbol{\sigma}}) + \\ &+\beta_{ex}\left(i(2\mathcal{A}\mathcal{B} - \mathcal{B}^2)\boldsymbol{J}\cdot(\boldsymbol{k}\times\boldsymbol{k}') + \mathcal{A}^2(\boldsymbol{J}\cdot\hat{\boldsymbol{\sigma}})(\boldsymbol{k}\cdot\boldsymbol{k}') - \mathcal{B}^2(\boldsymbol{J}\cdot\boldsymbol{k})(\hat{\boldsymbol{\sigma}}\cdot\boldsymbol{k}') - \mathcal{B}^2(\hat{\boldsymbol{\sigma}}\cdot\boldsymbol{k})(\boldsymbol{J}\cdot\boldsymbol{k}')\right).\end{aligned} \tag{22}$$

Being interested in the asymmetric scattering, one should drop all the k-dependent terms from Eq. 22 which are symmetric to $\boldsymbol{k} \longleftrightarrow \boldsymbol{k'}$. Indeed, the skew scattering rate Eq. 4 is quadratic in k in the leading order so only chiral terms of the form $\boldsymbol{k} \times \boldsymbol{k'}$ should be kept.

The exchange interaction part of the scattering potential also contributes to the longitudinal conductivity [42, 43]. When the impurities are spin-polarized the transport time from Eq. 6 becomes spin-dependent:

$$\frac{1}{\tau_{\uparrow,\downarrow}} = \frac{2\pi}{\hbar} n_i \nu (u_0 \pm \alpha_{ex} J)^2. \tag{23}$$

In the linear order with respect to u_X/u_0 the difference between the times is

$$\Delta\tau = \tau_\downarrow - \tau_\uparrow = \frac{4\alpha_{ex} J \tau}{u_0}, \quad \frac{1}{\tau} = \frac{2\pi}{\hbar} n_i \nu u_0^2. \tag{24}$$

Substituting the expressions for the scattering times into matrix A of Eq. 11, we get for the longitudinal conductivity σ_{xx} from Eq. 13:

$$\sigma_{xx} = \sigma_{xx}^\uparrow + \sigma_{xx}^\downarrow, \quad \sigma_{xx}^s = \frac{n_0 e^2 \tau_s}{2m}, \tag{25}$$

where n_0 is the electron concentration. Due to the difference between spin-up and spin-down conductivity $\sigma_{xx}^\uparrow \neq \sigma_{xx}^\downarrow$ an electrical current is accompanied with the spin current q_{xz} (spin along z flows in x direction) $q_{xz} = e^{-1}(\sigma_{xx}^\uparrow - \sigma_{xx}^\downarrow)E_x$.

We further calculate the skew scattering rate according to Eq. 4 with the matrix elements from Eq. 22. In the leading order with respect to u_X/u_0 we obtain

$$\begin{aligned} W_{kk'}^{ss'} &= -2\pi\nu u_0^2 (\boldsymbol{k} \times \boldsymbol{k'})_z (\sigma_z^{ss'} Z_0 + \delta_{ss'} Z_X), \\ Z_0 &= u_0(2\mathcal{AB} + \mathcal{B}^2), \\ Z_X &= \beta_{ex} J(2\mathcal{AB} - \mathcal{B}^2) + 2\alpha_{ex} J(2\mathcal{AB} + \mathcal{B}^2). \end{aligned} \tag{26}$$

Let us emphasize the appearance of two terms having different dependence on the electron spin state. The term related to the scalar potential contains the Pauli matrix σ_z and describes spin-dependent asymmetric scattering leading directly to the SHE. The second term with Z_X originates from the exchange interaction, being sensitive to the impurity magnetic moment rather than to the spin of the mobile electron. This type of the asymmetric scattering is spin-independent and it leads to the formation of the electric charge current even at vanishing electron spin polarization [25]. The spin-dependent contribution to the skew scattering leading to the transverse spin current and the spin-independent contributions are illustrated in Fig. 1.

The anomalous Hall conductivity can be obtained by combining τ_s and $W_{kk'}$ in Eqs. 14,15. The resulting expression for non-polarized electron gas is given by

$$\sigma_{yx} = \left(P_s\theta_0 + \theta_X - \theta_0 \frac{\Delta\tau}{\tau}\right) \frac{n_0 e^2 \tau}{m}, \quad P_s = \frac{n_\uparrow - n_\downarrow}{n_\downarrow + n_\uparrow} \tag{27}$$

where $\theta_{0,X} = Z_{0,X} \frac{2\pi}{3} \nu k_F^2$ have the meaning of the corresponding Hall angles, P_s is an electron spin polarization. Note that at $P_s = 0$ there are two terms in σ_{yx}. The first one θ_X originates from the asymmetry independent of the electron spin due to the exchange scattering, the second one θ_0 results from the conversion of the transverse spin current into electrical current due to $\tau_\uparrow \neq \tau_\downarrow$.

From the experimental point of view the anomalous Hall response in a semiconductor lightly doped with magnetic impurities turns out to be a combined effect of SOC in the host material and inner structure of the magnetic impurity. Note, that the admixture of the valence band is crucial for the effect. This is of no surprise for the conduction band electrons. However, as we will see further, the admixture of other bands will be also crucial for the skew scattering in the valence band, which is affected by SOC already in the zeroth order of the $\boldsymbol{k.p}$ theory.

B. Valence band

Let us now address the skew scattering of valence band holes populating Γ_8^v band. It would be rather natural to expect that the magnitude of skew scattering contribution to the AHE in Γ_8^v band would be much larger than that for the conduction band due to larger impact of SOC. However, as we demonstrate below, this argumentation fails as skew scattering rate remains of the same order of magnitude with respect to band-structure parameters. Moreover, a magnetic moment of the scatterer becomes of key importance to have any skew scattering at all.

Let us firstly consider skew scattering for the valence band holes described by Luttinger Hamiltonian in spherical approximation:

$$H = \frac{\hbar^2}{2m_0}\left((\gamma_1 + \frac{5}{2}\gamma_2)\boldsymbol{k}^2 - 2\gamma_2(\boldsymbol{k}\cdot\hat{\boldsymbol{\mathcal{J}}})^2\right), \tag{28}$$

here γ_1, γ_2 are Luttinger parameters, $\hat{\boldsymbol{\mathcal{J}}}$ are the matrices of angular momentum $3/2$. We use helicity basis for the heavy hole Ψ_{hh} and light hole Ψ_{lh} wavefunctions [44]:

$$\Psi_{lh,+}(\boldsymbol{k}) = \Psi_{lh,-}(-\boldsymbol{k}) = \begin{pmatrix} -\sqrt{3}\sin\frac{\theta}{2}\cos^2\frac{\theta}{2}e^{-\frac{3i\varphi}{2}} \\ (3\cos^2\frac{\theta}{2} - 2)\cos\frac{\theta}{2}e^{-\frac{i\varphi}{2}} \\ -(3\sin^2\frac{\theta}{2} - 2)\sin\frac{\theta}{2}e^{\frac{i\varphi}{2}} \\ \sqrt{3}\sin^2\frac{\theta}{2}\cos\frac{\theta}{2}e^{\frac{3i\varphi}{2}} \end{pmatrix} \tag{29}$$

$$\Psi_{hh,+}(\boldsymbol{k}) = \Psi_{hh,-}(-\boldsymbol{k}) = \begin{pmatrix} \cos^3\frac{\theta}{2}e^{-\frac{3i\varphi}{2}} \\ \sqrt{3}\sin\frac{\theta}{2}\cos^2\frac{\theta}{2}e^{-\frac{i\varphi}{2}} \\ \sqrt{3}\sin^2\frac{\theta}{2}\cos\frac{\theta}{2}e^{\frac{i\varphi}{2}} \\ \sin^3\frac{\theta}{2}e^{\frac{3i\varphi}{2}} \end{pmatrix}, \tag{30}$$

These wavefunctions are the eigenvectors of the helicity operator $\hat{\eta} = (\boldsymbol{k}/k)\cdot\hat{\boldsymbol{\mathcal{J}}}$. The notation $\pm$ stands for the positive or negative helicity, namely $\langle\Psi_{hh,\pm}|\hat{\eta}|\Psi_{hh,\pm}\rangle =$

$\pm 3/2$ and $\langle \Psi_{lh,\pm}|\hat{\eta}|\Psi_{lh,\pm}\rangle = \pm 1/2$. In this basis the scattering times for the light holes and heavy holes entering matrix A (see Eq. 11) are equal:

$$\tau_{lh,\pm}^{-1} = \tau_{hh,\pm}^{-1} = \frac{8\pi^2}{\hbar} n_i \langle \nu \rangle u_0^2, \quad \langle \nu \rangle = \frac{\nu_{lh} + \nu_{hh}}{2}. \tag{31}$$

The scattering asymmetry matrix B is explicitly written in the Supplemental. We note here that the asymmetric scattering rate $W_{kk'}^{\nu\mu}$ contains multiple angular harmonics. Only the first angular harmonics with $l = 1$ are relevant for the electrical current, while higher harmonics could contribute to other physical phenomena. The rates describing skew scattering in all the scattering channels appear to have the form

$$W = \zeta \langle \nu \rangle u_0^2 \beta_{ex} J (Y_x' Y_y - Y_y' Y_x), \tag{32}$$

ζ being a numerical factor, given explicitly in the Supplemental. Note that these rates are linear in β_{ex}, so that there is no skew scattering without the exchange part of the impurity potential. Moreover, even in the presence of the exchange interaction the electric Hall current calculated by substituting A, B matrices into Eq. 15 turns out to be zero as the contribution from different channels cancel each other out.

Let us note that the skew-scattering rates generally transform when changing the wavefunction basis. In particular, using the basis for Γ_8^v as in Ref. [45] (rather than fixed chirality basis) we find that the matrix of asymmetry turns out to be zero $B = 0$ so the absence of AHE can be seen in this case right from the very beginning.

Since there is no skew scattering for the Luttinger Hamiltonian we further consider Kane model and analyze whether taking into account $\boldsymbol{k}.\boldsymbol{p}$ admixture of remote bands would give rise to a finite skew-scattering of the valence band holes. Firstly, let us take into account the admixture of the Γ_6^c states of the conductance band. The heavy holes are not affected $\delta\Psi_{hh,+} = \delta\Psi_{hh,-} = 0$, for the light-holes the linear in k correction to Γ_8^v wavefunction appear:

$$\begin{aligned} \delta\Psi_{lh,+} &= \frac{ikP}{E_0}\frac{\sqrt{6}}{3}\left(\cos\frac{\theta}{2}e^{-\frac{i\varphi}{2}}|S\uparrow\rangle + \sin\frac{\theta}{2}e^{\frac{i\varphi}{2}}|S\downarrow\rangle\right) \\ \delta\Psi_{lh,-} &= \frac{kP}{E_0}\frac{\sqrt{6}}{3}\left(\cos\frac{\theta}{2}e^{\frac{i\varphi}{2}}|S\downarrow\rangle - \sin\frac{\theta}{2}e^{-\frac{i\varphi}{2}}|S\uparrow\rangle\right) \end{aligned} \tag{33}$$

Using Eq. 19 one verifies $\langle \Psi_{hh,+}|\Psi_{ks}\rangle = \langle \Psi_{hh,-}|\Psi_{ks}\rangle = 0$, so the $\boldsymbol{k}.\boldsymbol{p}$ coupling between Γ_6^c and Γ_8^v bands is only via electron-light hole states. Similarly to the conduction band states considered in the previous section, the admixture of the Γ_6^c states to the light holes gives rise to the skew-scattering, the corresponding asymmetric rates are given by

$$\begin{aligned} W_{lh+,lh+}^{(1)} = W_{lh+,lh-}^{(1)} = W_{lh-,lh-}^{(1)} = \\ = -\frac{2\pi^2\langle \nu \rangle kk'P^2}{9E_0^2} u_0^2(\alpha_{ex} + 10\beta_{ex})J. \end{aligned} \tag{34}$$

We note that skew-scattering rates are nonzero only if an impurity has an inner magnetic moment. The sign of the scattering asymmetry is unique for all scattering channels within the light-hole sector as it is determined by the impurity magnetic moment.

The appearance of the same sign skew scattering is in contrast to the case of electrons from Γ_6^c; in particular it implies that the conductivity difference mechanism of the anomalous Hall resistivity driven by the scalar part of the impurity potential is suppressed for the light holes. Using Eqs. 14,15 we derive the following expression for the electric Hall current

$$j_y = e^2 E_x \frac{(2m_{lh}\varepsilon_F)^3}{8\pi^5\hbar^7 n_i}\left(\frac{P}{E_0}\right)^2 \frac{(\alpha_{ex} + 10\beta_{ex})\,J}{18\langle \nu \rangle u_0^2}. \tag{35}$$

Interestingly, the leading contribution to the AHE stems entirely from the light holes species. Besides, the magnitude of the AHE for the holes and for the electrons appears to be comparable despite the itinerant SOC of the Γ_8^v states.

A skew-scattering for a heavy-hole state is also possible but it emerges in a higher order in k. In particular, we considered 14-band $k.p$ model and took into account the admixture of p-like (X', Y', Z') conduction band states $\Gamma_{7,8}^c$ The corresponding wave-functions are summarized in the Supplemental. We take into account only $Q = (i\hbar/m)\langle X'|\hat{p}_y|Z\rangle$, E_0' and Δ parameters (see Fig. 2) and neglect Δ^- as the latter appears to give no contribution to the asymmetric scattering rates:

$$W^{(1)}_{lh+,lh+} = W^{(1)}_{lh-,lh-} = W^{(1)}_{lh+,lh-} = u_0^2 \Big(\frac{2}{9}\pi^2 \left(\frac{P}{E_0}\right)^2 \langle\nu\rangle k_{lh}^2 \left(\alpha_{ex} + 10\beta_{ex}\right) J + \\ + \frac{\langle\nu\rangle}{135}\pi^2 \left(\frac{Q}{E_0' + \Delta}\right)^2 k_{lh}^2 \left(2\beta_{ex} - \gamma_{ex}\right) J + \frac{2}{27}\pi^2 \left(\frac{Q}{E_0'}\right)^2 \langle\nu\rangle k_{lh}^2 \left(10\beta_{ex} + \gamma_{ex}\right) J \Big) (Y_x' Y_y - Y_y' Y_x) \tag{36}$$

$$W^{(1)}_{lh+,hh+} = W^{(1)}_{lh-,hh-} = W^{(1)}_{lh+,hh-} = W^{(1)}_{lh-,hh+} = u_0^2 \left(\frac{\langle\nu\rangle}{15}\pi^2 \left(\frac{Q}{E_0' + \Delta}\right)^2 k_{hh} k_{lh} \left(2\beta_{ex} - \gamma_{ex}\right) J \right) (Y_x' Y_y - Y_y' Y_x) \tag{37}$$

$$W^{(1)}_{hh+,hh+} = W^{(1)}_{hh-,hh-} = W^{(1)}_{hh+,hh-} = u_0^2 \left(\frac{3}{5}\pi^2 \left(\frac{Q}{E_0' + \Delta}\right)^2 \langle\nu\rangle k_{hh}^2 \left(2\beta_{ex} - \gamma_{ex}\right) J \right) (Y_x' Y_y - Y_y' Y_x) \tag{38}$$

The magnetic component of the scattering potential eventually gives rise to the Hall current, which would be otherwise zero in the case of non-magnetic scatterers. Also, the matrix element $\gamma_{ex} = \langle X'|\hat{J}_{ex}|X'\rangle$ of the exchange interaction for the higher conductance band appears in the expression for the symmetrical rates. Thus, the admixture of the conduction band states to the valence band states is an important factor behind the formation of AHE driven by holes in zinc-blend semiconductors.

We would like to propose that the discovered suppression of the skew scattering of the heavy holes on non-magnetic centers is likely to contribute to the known superlinear transverse vs longitudinal resistance scaling in p-type (Ga,Mn)As [46, 47].

IV. QUANTUM WELLS

In this section we turn to low-dimensional systems and investigate the skew scattering features for the degenerate electron gas (2DEG) in a quantum well (QW).

A. Rashba Hamiltonian

It is worth noting that there are different scenarios for the material SOC to affect the electron dynamics in a QW. A particularly important one is due to the so-called structure inversion asymmetry (SIA) [39, 48], when due to asymmetric potential profile of the QW linear in the electron momentum terms appear in the effective Rashba Hamiltonian:

$$H_R = \frac{\hbar^2 k^2}{2m} + \lambda_R \left(\sigma_x k_y - \sigma_y k_x\right). \tag{39}$$

Here m is the in-plane effective mass, λ_R is the strength of the Rashba-type SOC. The eigen-wavefunctions $\Psi_\pm = e^{i\boldsymbol{kr}} u_\pm$ corresponding to energies $\varepsilon_\pm = \hbar^2 k^2/2m \pm \lambda_R k$ are given by

$$u_\pm = \frac{1}{\sqrt{2}} \begin{pmatrix} \pm i e^{-i\varphi} \\ 1 \end{pmatrix}. \tag{40}$$

We note that in this model electrons exhibit strong spin-momentum locking, i.e. the orientation of $\boldsymbol{S}_k = (\boldsymbol{e}_z \times \boldsymbol{k})/2$ is determined by $\boldsymbol{k}$.

Spin transport in systems with Rashba term are being intensively studied [6, 7, 49]. It is now established that the skew-scattering induced AHE can behave differently depending on multiple factors. In particular, for the Rashba ferromagnet model, when in addition to Eq. 39 a magnetic Zeeman spin splitting is taken into account, the skew scattering depends crucially on the position on the Fermi energy. When both spin subbands are partially populated the third order contributions to the asymmetric scattering rates from Eq. 4 vanishes [16, 18, 50] and one has to go in higher orders of the Born approximation [17, 38]. For a single spin subband at the Fermi energy the skew scattering is typically preserved in the third order [13]. On the contrary, considering a nonmagnetic system (meaning when no Zeeman spin splitting is taken into account) the skew scattering due to a scalar impurity does not appear at all. However, as we demonstrate below, the absence of skew scattering in 2D for this simplified model does not have a universal character and its properties can be strongly modified by various microscopic factors.

For instance, in full analogy with Γ_8^v states considered in Sec. III B, the electrons described by H_R scatter asymmetrically if the scatterer potential has an exchange part due to the impurity spin. Indeed, let us consider a short-range scattering potential of the form

$$\hat{V} = (u_0 + u_X J \hat{\sigma}_z)\delta(\boldsymbol{r}), \tag{41}$$

here u_0 and u_X correspond to the electrostatic and exchange interaction, respectively. Using the eigenstates from Eq. 40 we get the following expression for the skew scattering rates

$$B = \pi u_X (u_0^2 - u_X^2 J^2)\langle\nu\rangle \begin{pmatrix} \nu_+ & -\nu_- \\ -\nu_+ & \nu_- \end{pmatrix}, \tag{42}$$

where $\langle\nu\rangle = (\nu_+ + \nu_-)/2$ is an average DOS at the Fermi energy E, the DOS $\nu_\pm$ in each subband is given by

$$\nu_\pm = \frac{m}{2\pi\hbar^2}\left[1 \mp \left(1+\frac{2\hbar^2 E}{m\alpha^2}\right)^{-1/2}\right]. \qquad (43)$$

Thus, we attest to the appearance of finite skew scattering rates due to nonzero exchange interaction constant u_X.

In contrast to the the Luttinger Hamiltonian case considered above, here the asymmetry in the scattering rates does lead to the appearance of finite anomalous Hall conductivity. Indeed, let us calculate the electric current for this model. We keep to the strong SOC regime in the sense that we assume that the broadening of DOS due to electron scattering does not exceed the Rashba spin splitting $\lambda_R k_F \tau/\hbar \gg 1$. In this case the electron transport can be described using the approach of Sec. II with the the unperturbed expressions for $\nu_\pm$ from Eq. 43 and exact Rashba spectrum from Eq. 39. Calculating the longitudinal part of the collision integral using the eigenstates Eq. 40 we obtain

$$A = \begin{pmatrix} -\tau_R^{-1}+\gamma_+ & -\gamma_- \\ -\gamma_+ & -\tau_R^{-1}+\gamma_- \end{pmatrix},$$
$$\tau_R^{-1} \approx \frac{2\pi}{\hbar} n_i u_0^2 \langle\nu\rangle, \quad \gamma_\pm = \frac{2\pi}{\hbar} n_i \frac{u_0^2}{4}\nu_\pm, \qquad (44)$$

here the parameters $\tau_R^{-1}, \gamma_\pm$ are given in the leading order with respect to u_X/u_0. Using Eqs. 14,15 we calculate the Hall current

$$j_y = e^2 E_x 2\pi v_F^2 \tau_R u_X J(\nu_+ - \nu_-)^2. \qquad (45)$$

Therefore, in the presence of magnetic scatterers the transverse current is not canceled out restoring AHE for the 2D Rashba-type Hamiltonian. It is important to emphasize that apart from the exchange interaction strength the Hall current is also proportional to the difference in DOS for the two subbands $\nu_+ - \nu_-$ at the Fermi level. The strong SOC regime assumed in this calculation ensures $\nu_+ \neq \nu_-$, otherwise the disorder induced smearing of DOS would eliminate the spin-dependent part $\nu_+ \approx \nu_-$ leading to the vanishing of the Hall current.

B. Size-quantization effects

Let us consider another microscopic scenario capable to restore the significance of the skew scattering in semiconductor QW systems. Besides the Rashba Hamiltonian model, the SOC can be explicitly inherited by QW conductive band electrons from the bulk band structure considered in detail in Sec. III B. Indeed, considering the size-quantization effect along the QW growth axis of electron states given by Eq. 19 one can derive [51] the following expressions for the electron wavefunctions in a QW

$$\Psi_{s,\boldsymbol{k}}(\boldsymbol{r}) = c_k e^{i\boldsymbol{k}\cdot\boldsymbol{r}}(u_s(z)\cdot S + \boldsymbol{v}_{s\boldsymbol{k}}(z)\cdot\boldsymbol{R}), \qquad (46)$$
$$\boldsymbol{v}_{s\boldsymbol{k}} = i(\mathcal{A}\boldsymbol{K} - i\mathcal{B}\boldsymbol{\sigma}\times\boldsymbol{K})u_s(z), \qquad (47)$$

where $\boldsymbol{K} = (\boldsymbol{k}, -i\partial_z)$ and $u_s(z) = \varphi(z)|s\rangle$ contains an envelope wavefunction reflecting the size quantization $\varphi(z)$. The dominant part of the matrix element of the scattering potential $u_0(\boldsymbol{r})$ calculated using the wavefunctions from above can be expressed as [51]

$$V_{kk'} = V_0(1 + a\boldsymbol{\sigma}((\boldsymbol{k}+\boldsymbol{k'})\times\boldsymbol{e_z})),$$
$$a = (2\mathcal{A}\mathcal{B}+\mathcal{B}^2)\int u_0\varphi^*(z)\frac{\partial}{\partial z}\varphi(z). \qquad (48)$$

where $a = (2\mathcal{A}\mathcal{B}+\mathcal{B}^2)\langle\varphi|u_0\partial_z|\varphi\rangle_z$, here the average goes over the QW growth axis z. Using this matrix element we calculate the skew scattering rates from Eq. 4

$$W_{kk'}^{ss'} = 2\pi\nu V_0^3 a^2 \sigma_z^{ss'}(\boldsymbol{k}\times\boldsymbol{k'})_z. \qquad (49)$$

In fact, the obtained expression mimics the skew scattering rates of Γ_6^c electron in bulk but the coefficient a now contains information on the QW size quantization. In particular, when impurities do not posses an additional magnetic moment (hence no exchange interaction part), the emergence of skew scattering visible from Eq. 49 is already sufficient to give rise to nonzero spin Hall conductivity. Indeed, performing the standard procedure according to Eq. 14 we arrive at the following expression for the Hall current j_H^s for electrons with spin projection s

$$j_H^s = -\frac{e^2 E_x \hbar\nu v}{n_i V_0}(k_F a)^2. \qquad (50)$$

The non-vanishing spin Hall current can be converted into the electric transverse signal upon non-equilibrium carrier spin polarization.

The presented analysis reveals that in the 2D case the skew scattering is not universally suppressed but rather depends on the microscopic details of the SOC induced conduction band states and the scatterer structure. Moreover, for the Rashba SOC the skew scattering emerges when an impurity possesses a magnetic moment.

V. SUMMARY

We have clarified the important differences in microscopic mechanisms and emergent features of the skew scattering of conductance band electrons and valence band holes on non-magnetic and paramagnetic centers in zinc-blende semiconductors. As we have demonstrated the effect of SOC on the band structure and the skew scattering are not directly related although based on the same physics of SOC. In particular, for a bulk semiconductor the skew scattering is determined by the wavefunction properties. While SOC leads to a rather large splitting of the spectra for the valence band, the skew scattering is suppressed for the heavy holes. For the light holes it is of a similar magnitude as for the conduction band electrons subject to $\boldsymbol{k.p}$ driven coupling between the bands. We also demonstrated that presence of a magnetic impurity qualitatively modifies the skew scattering properties. Most brightly it is seen for the 3D holes and 2D Rashba electrons. In these cases the scattering on a magnetic center allows for the asymmetry leading to the extrinsic contribution to the anomalous Hall effect otherwise suppressed. The exchange interaction between the magnetic moment of the scatterer and the incident carrier spin leads to the spin-independent scattering asymmetry, hence, to the anomalous Hall effect even in the absence of the spin polarization of the mobile carriers.

Our findings enrich the understanding of the spin-dependent transport and motivate further experimental probe of the revealed intricate properties of the skew scattering in semiconductors.

ACKNOWLEDGEMENTS

I.V.R., E.L. acknowledge Academy of Finland (grant No. 318500), I.V.R. is grateful to Weizmann Institute of Science for support and hospitality, K.S.D., I.V.R. and M.A.R thank the Foundation for the Advancement of Theoretical Physics and Mathematics "BASIS". We are grateful to Allan H. MacDonald for valuable discussions.

DATA AVAILABILITY

Data sharing is not applicable to this article as no new data were created or analyzed in this study.

Further calculation details and intermediate formulas are given in the Supplemental Material [52].

[1] B. T. Zhou, K. Taguchi, Y. Kawaguchi, Y. Tanaka, and K. T. Law, Spin-orbit coupling induced valley hall effects in transition-metal dichalcogenides, Communications Physics **2**, 1 (2019).

[2] M. Onga, Y. Zhang, T. Ideue, and Y. Iwasa, Exciton hall effect in monolayer mos2, Nature materials **16**, 1193 (2017).

[3] C. Song, R. Zhang, L. Liao, Y. Zhou, X. Zhou, R. Chen, Y. You, X. Chen, and F. Pan, Spin-orbit torques: materials, mechanisms, performances, and potential applications, Progress in Materials Science , 100761 (2020).

[4] A. Manchon, J. Železný, I. M. Miron, T. Jungwirth, J. Sinova, A. Thiaville, K. Garello, and P. Gambardella, Current-induced spin-orbit torques in ferromagnetic and antiferromagnetic systems, Rev. Mod. Phys. **91**, 035004 (2019).

[5] A. Soumyanarayanan, N. Reyren, A. Fert, and C. Panagopoulos, Emergent phenomena induced by spin–orbit coupling at surfaces and interfaces, Nature **539**, 509 (2016).

[6] N. Nagaosa, J. Sinova, S. Onoda, A. H. MacDonald, and N. P. Ong, Anomalous Hall effect, Rev. Mod. Phys. **82**, 1539 (2010).

[7] J. Sinova, S. Valenzuela, J. Wunderlich, C. H. Back, and T. Jungwirth, Spin Hall effects, Rev. Mod. Phys. **87**, 1213 (2015).

[8] J. Smit, The spontaneous hall effect in ferromagnetics i, Physica **21**, 877 (1955).

[9] J. Smit, The spontaneous hall effect in ferromagnetics ii, Physica **24**, 39 (1958).

[10] A. Fert and O. Jaoul, Left-right asymmetry in the scattering of electrons by magnetic impurities, and a Hall effect, Phys. Rev. Lett. **28**, 303 (1972).

[11] A. Fert and A. Friederich, Skew scattering by rare-earth impurities in silver, gold, and aluminum, Physical Review B **13**, 397 (1976).

[12] A. Fert, A. Friederich, and A. Hamzic, Hall effect in dilute magnetic alloys, Journal of Magnetism and Magnetic Materials **24**, 231 (1981).

[13] N. A. Sinitsyn, A. H. MacDonald, T. Jungwirth, V. K. Dugaev, and J. Sinova, Anomalous hall effect in a two-dimensional dirac band: The link between the kubo-streda formula and the semiclassical boltzmann equation approach, Phys. Rev. B **75**, 045315 (2007).

[14] V. N. Abakumov and I. N. Yassievich, Anomalous Hall effect for polarized electrons in semiconductors, Soviet JETP **34**, 1375 (1972).

[15] M. I. Dyakonov and V. I. Perel, Current-induced spin orientation of electrons in semiconductors, Physics Letters A **35**, 459 (1971).

[16] M. Borunda, T. S. Nunner, T. Lück, N. A. Sinitsyn, C. Timm, J. Wunderlich, T. Jungwirth, A. H. MacDonald, and J. Sinova, Absence of skew scattering in two-dimensional systems: Testing the origins of the anomalous Hall effect, Phys. Rev. Lett. **99**, 066604 (2007).

[17] A. A. Kovalev, K. Výborný, and J. Sinova, Hybrid skew scattering regime of the anomalous hall effect in rashba systems: Unifying keldysh, boltzmann, and kubo formalisms, Phys. Rev. B **78**, 041305 (2008).

[18] N. A. Sinitsyn, Semiclassical theories of the anomalous Hall effect, Journal of Physics: Condensed Matter **20**, 023201 (2007).

[19] B. Zimmermann, K. Chadova, D. Ködderitzsch, S. Blügel, H. Ebert, D. V. Fedorov, N. H. Long, P. Mavropoulos, I. Mertig, Y. Mokrousov, and M. Gradhand, Skew scattering in dilute ferromagnetic alloys, Phys. Rev. B **90**, 220403 (2014).

[20] B. Zimmermann, N. H. Long, P. Mavropoulos, S. Blügel, and Y. Mokrousov, Influence of complex disorder on skew-scattering hall effects in $L1_0$-ordered FePt alloy, Phys. Rev. B **94**, 060406 (2016).

[21] A. Hönemann, C. Herschbach, D. V. Fedorov, M. Gradhand, and I. Mertig, Absence of strong skew scattering in crystals with multi-sheeted fermi surfaces, Journal of Physics: Condensed Matter **31**, 085803 (2019).

[22] G.-Y. Guo, S. Maekawa, and N. Nagaosa, Enhanced spin Hall effect by resonant skew scattering in the orbital-dependent Kondo effect, Phys. Rev. Lett. **102**, 036401 (2009).

[23] D. Maryenko, A. Mishchenko, M. Bahramy, A. Ernst, J. Falson, Y. Kozuka, A. Tsukazaki, N. Nagaosa, and M. Kawasaki, Observation of anomalous Hall effect in a non-magnetic two-dimensional electron system, Nature communications **8**, 1 (2017).

[24] J. Kondo, Anomalous Hall effect and magnetoresistance of ferromagnetic metals, Progress of Theoretical Physics **27**, 772 (1962).
[25] M. A. Rakitskii, K. S. Denisov, I. V. Rozhansky, and N. S. Averkiev, Fingerprints of the electron skew scattering on paramagnetic impurities in semiconductor systems, Applied Physics Letters **118**, 032105 (2021).
[26] I. A. Ado, I. A. Dmitriev, P. M. Ostrovsky, and M. Titov, Anomalous hall effect in a 2d rashba ferromagnet, Phys. Rev. Lett. **117**, 046601 (2016).
[27] S. Onoda, N. Sugimoto, and N. Nagaosa, Intrinsic versus extrinsic anomalous hall effect in ferromagnets, Phys. Rev. Lett. **97**, 126602 (2006).
[28] T. Jungwirth, Q. Niu, and A. H. MacDonald, Anomalous hall effect in ferromagnetic semiconductors, Phys. Rev. Lett. **88**, 207208 (2002).
[29] S. Liu, N. Horing, and X. Lei, Long range scattering effects on spin hall current in p-type bulk semiconductors, Physical Review B **73** (2005).
[30] P. Kleinert and V. Bryksin, Theory of spin-hall transport of heavy holes in semiconductor quantum wells, J. Phys.: Condens. Matter **18** (2006).
[31] W. Zhi-Gang and Z. Ping, Anomalous hall effect of heavy holes in iii-v semiconductor quantum wells, Chinese Physics **16**, 517 (2007).
[32] J. Sinova, T. Jungwirth, J. Kučera, and A. H. MacDonald, Infrared magneto-optical properties of (iii,mn)v ferromagetic semiconductors, Phys. Rev. B **67**, 235203 (2003).
[33] A. A. Kovalev, J. Sinova, and Y. Tserkovnyak, Anomalous hall effect in disordered multiband metals, Phys. Rev. Lett. **105**, 036601 (2010).
[34] S. H. Chun, Y. S. Kim, H. K. Choi, I. T. Jeong, W. O. Lee, K. S. Suh, Y. S. Oh, K. H. Kim, Z. G. Khim, J. C. Woo, and Y. D. Park, Interplay between carrier and impurity concentrations in annealed ga$_{1-x}$mn$_x$As: Intrinsic anomalous hall effect, Phys. Rev. Lett. **98**, 026601 (2007).
[35] L. N. Oveshnikov, V. A. Kulbachinskii, A. B. Davydov, B. A. Aronzon, I. V. Rozhansky, N. S. Averkiev, K. I. Kugel, and V. Tripathi, Berry phase mechanism of the anomalous Hall effect in a disordered two-dimensional magnetic semiconductor structure, Scientific Reports **5**, 17158 (2015).
[36] D. Chiba, A. Werpachowska, M. Endo, Y. Nishitani, F. Matsukura, T. Dietl, and H. Ohno, Anomalous hall effect in field-effect structures of (ga,mn)as, Phys. Rev. Lett. **104**, 106601 (2010).
[37] T. Jungwirth, Q. Niu, and A. H. MacDonald, Anomalous hall effect in ferromagnetic semiconductors, Phys. Rev. Lett. **88**, 207208 (2002).
[38] A. A. Kovalev, Y. Tserkovnyak, K. Výborný, and J. Sinova, Transport theory for disordered multiple-band systems: Anomalous hall effect and anisotropic magnetoresistance, Phys. Rev. B **79**, 195129 (2009).
[39] R. Winkler, *Spin-orbit coupling effects in two-dimensional electron and hole systems*, Springer tracts in modern physics (Springer, Berlin, 2003).
[40] V. Abakumov and I. Yassievich, Anomalous hall effect for polarized electrons in semiconductors, Soviet Journal of Experimental and Theoretical Physics **34**, 1375 (1972).
[41] E. L. Ivchenko and G. Pikus, *Superlattices and other heterostructures: symmetry and optical phenomena*, Vol. 110 (Springer Science & Business Media, 2012).
[42] M. Foygel and A. G. Petukhov, Scattering by atomic spins and magnetoresistance in dilute magnetic semiconductors, Phys. Rev. B **76**, 205202 (2007).
[43] S. D. Ganichev, S. A. Tarasenko, V. V. Bel'kov, P. Olbrich, W. Eder, D. R. Yakovlev, V. Kolkovsky, W. Zaleszczyk, G. Karczewski, T. Wojtowicz, and D. Weiss, Spin currents in diluted magnetic semiconductors, Phys. Rev. Lett. **102**, 156602 (2009).
[44] J. Schliemann, Theoretical study of interacting hole gas in p-doped bulk iii-v semiconductors, Physical Review B **74** (2006).
[45] P. G. Ivchenko, E.L., *Superlattices and Other Heterostructures* (Springer, 1997).
[46] M. Glunk, J. Daeubler, W. Schoch, R. Sauer, and W. Limmer, Scaling relation of the anomalous hall effect in (ga,mn)as, Phys. Rev. B **80**, 125204 (2009).
[47] D. Chiba, A. Werpachowska, M. Endo, Y. Nishitani, F. Matsukura, T. Dietl, and H. Ohno, Anomalous hall effect in field-effect structures of (ga,mn)as, Phys. Rev. Lett. **104**, 106601 (2010).
[48] Y. A. Bychkov and É. I. Rashba, Properties of a 2D electron gas with lifted spectral degeneracy, JETP lett **39**, 78 (1984).
[49] A. Manchon, H. Koo, J. Nitta, S. Frolov, and R. Duine, New perspectives for Rashba spin–orbit coupling, Nature materials **14**, 871 (2015).
[50] T. S. Nunner, N. A. Sinitsyn, M. F. Borunda, V. K. Dugaev, A. A. Kovalev, A. Abanov, C. Timm, T. Jungwirth, J.-i. Inoue, A. H. MacDonald, and J. Sinova, Anomalous hall effect in a two-dimensional electron gas, Phys. Rev. B **76**, 235312 (2007).
[51] N. Averkiev, L. Golub, and M. Willander, Spin relaxation anisotropy in two-dimensional semiconductor systems, Journal of physics: condensed matter **14**, R271 (2002).
[52] See Supplemental Material at [URL will be inserted by publisher] for calculation details and intermediate formulas.

Supplemental materials for: Intricate features of electron and hole skew scattering in semiconductors

M. A. Rakitskii,[1] K. S. Denisov,[1] E. Lähderanta,[1] and I. V. Rozhansky[1,2,*]

[1] *LUT University, FI-53851 Lappeenranta, Finland*

[2] *École Polytechnique, Institut Polytechnique de Paris, 91128 Palaiseau, France*

(Dated: February 8, 2023)

I. DEFINITIONS

For the convenience we give here some definitions used throughout the paper and Supplemental material:
m — electron effective mass,
$\boldsymbol{v}_s$ — electron velocity in subband s,
ν_s — density of states in subband s,
n_i — impurity concentration,
$\hat{V}$ — scattering potential,
δf^s — non-equilibrium carrier distribution function in subband s,
The asymmetric term in the scattering rate in third order according to $\hat{V}$ is given by:

$$W_{kk'}^{ss'} = 2\pi \sum_l \nu_l(E) \langle \mathrm{Im}(V_{k'k}^{s's} V_{kq}^{sl} V_{qk'}^{ls'}) \rangle_{\Omega_q}, \tag{S1}$$

where $\langle \dots \rangle_{\Omega_q}$ denotes an average over wavevector $\boldsymbol{k}$ directions.

It proves useful to expand physical quantities in first order spherical harmonics $Y_{x,y,z}$, so we define $w_{ss'}$, $u_{ss'}$ and $f^s_{x,y,z}$ as coefficients in spherical harmonics expansion:

$$W_{kk'}^{ss'} = w_{ss'}(Y'_x Y_y - Y'_y Y_x),$$
$$|V_{kk'}^{ss'}|^2 = const + u_{ss'}(Y_x Y'_x + Y_y Y'_y + Y_z Y'_z), \tag{S2}$$
$$\delta f^s = f_x^s Y_x + f_y^s Y_y + f_z^s Y_z, \tag{S3}$$

where spherical harmonic functions with prime symbol depend on φ' and θ' angles of wavevector $\boldsymbol{k'}$ direction rather than on φ and θ of wavevector $\boldsymbol{k}$. We also introduce quantum scattering time in s-subband:

$$\frac{1}{\tau_s} = \frac{2\pi}{\hbar} n_i \sum_{s'\boldsymbol{k'}} \delta(\varepsilon_k^s - \varepsilon_{k'}^{s'}) |V_{k'k}^{s's}|^2. \tag{S4}$$

For m subbands, we define velocities vector V, vectors of coefficients F_x and F_y, and matrices A and B:

$$V = \begin{pmatrix} v_1 \\ \vdots \\ v_m \end{pmatrix}, \quad F_x = \begin{pmatrix} f_x^1 \\ \vdots \\ f_x^m \end{pmatrix}, \quad F_y = \begin{pmatrix} f_y^1 \\ \vdots \\ f_y^m \end{pmatrix},$$
$$A_{ss'} = \nu_{s'} u^{ss'} - \delta_{ss'} {\tau_s}^{-1}, \qquad B_{ss'} = \nu_{s'} w^{ss'}. \tag{S5}$$

For each subband s one can write the Boltzmann kinetic equation:

$$eE_x v_x^s \frac{\partial f^0}{\partial \varepsilon} = \sum_{s'} \nu' u^{ss'} (Y_x f_x^{s'} + Y_y f_y^{s'} + Y_z f_z^{s'}) - \frac{1}{\tau_s}(Y_x f_x^s + Y_y f_y^s + Y_z f_z^s) + \sum_{s'} \nu' w^{ss'} (Y_y f_x^{s'} - Y_x f_y^{s'}). \tag{S6}$$

* rozhansky@gmail.com

There is one angular harmonic at the left-hand side $v_x^s = v_s Y_x$ and three at the right-hand side. So expanding (S6) into three for each angular harmonic we get

$$\begin{aligned} eE_x v_s \frac{\partial f^0}{\partial \varepsilon} &= \sum_{s'} \nu' u^{ss'} f_x^{s'} - f_x^s {\tau_s}^{-1} - \sum_{s'} \nu' w^{ss'} f_y^{s'}, \\ 0 &= \sum_{s'} \nu' u^{ss'} f_y^{s'} - f_y^s {\tau_s}^{-1} + \sum_{s'} \nu' w^{ss'} f_x^{s'}, \\ 0 &= \sum_{s'} \nu' u^{ss'} f_z^{s'} - f_z^s {\tau_s}^{-1}. \end{aligned} \tag{S7}$$

The third equation has trivial solution, and the first two can be written as a matrix equation $2n_s \times 2n_s$ (n_s is the number of spin subbands):

$$eE_x \frac{\partial f^0}{\partial \varepsilon} \begin{pmatrix} V \\ 0 \end{pmatrix} = \begin{pmatrix} A & -B \\ B & A \end{pmatrix} \begin{pmatrix} F_x \\ F_y \end{pmatrix}, \tag{S8}$$

which gives following result for F_y coefficients

$$F_y = -A^{-1} B F_x = -eE_x \frac{\partial f^0}{\partial \varepsilon} A^{-1} B A^{-1} V. \tag{S9}$$

Having an explicit expression for f_y^s coefficients, the transverse electric current can be computed:

$$j_y = e \sum_s \int \langle v_y^s \delta f^s \rangle_\Omega \nu_s \, \mathrm{d}\,\varepsilon = e \sum_s \int v_s f_y^s \nu_s \, \mathrm{d}\,\varepsilon = e^2 E_x \sum_s \nu_s v_s (A^{-1} B A^{-1} V)_s. \tag{S10}$$

In $\boldsymbol{k}.\boldsymbol{p}$ model calculations we will use the canonical basis for valence band states at Γ_8 point defined as follows:

$$|1\rangle = -\frac{1}{\sqrt{2}}(X\uparrow + iY\uparrow), \qquad |2\rangle = -\frac{1}{\sqrt{6}}(X\downarrow + iY\downarrow) + \sqrt{\frac{2}{3}} Z\uparrow, \tag{S11}$$

$$|3\rangle = \frac{1}{\sqrt{6}}(X\uparrow - iY\uparrow) + \sqrt{\frac{2}{3}} Z\downarrow, \qquad |4\rangle = \frac{1}{\sqrt{2}}(X\downarrow - iY\downarrow), \tag{S12}$$

$$|5\rangle = \frac{1}{\sqrt{3}}(X\downarrow + iY\downarrow + Z\uparrow), \qquad |6\rangle = -\frac{1}{\sqrt{3}}(X\uparrow - iY\uparrow - Z\downarrow). \tag{S13}$$

II. WAVEFUNCTIONS

A. Conduction band

Electron wavefunction in bulk zinc-blende semiconductor is calculated with k-p method, taking into account admixture of valence band wavefunctions, and can be written in the following form:

$$\Psi_{ks} = e^{i\boldsymbol{kr}} \Big(S + i\boldsymbol{R}\big(\mathcal{A}\boldsymbol{k} - i\mathcal{B}(\hat{\boldsymbol{\sigma}} \times \boldsymbol{k})\big) \Big) |\chi_s\rangle, \tag{S14}$$

where material parameters $\mathcal{A}$ and $\mathcal{B}$ are defined as

$$\mathcal{A} = P \frac{3E_0 + 2\Delta}{3E_0(E_0 + \Delta)}, \quad \mathcal{B} = -P \frac{\Delta}{3E_0(E_0 + \Delta)}, \quad P = \frac{i\hbar}{m} \langle S | \hat{p}_x | X \rangle. \tag{S15}$$

We consider a scattering potential consisting of scalar and magnetic terms, both of them are short-ranged and have matrix elements u_0, α_{ex} and β_{ex} [S1].

$$\hat{V} = u(\boldsymbol{r})\hat{I} + \hat{u}_X(\boldsymbol{r}) \boldsymbol{J} \cdot \hat{\sigma}, \tag{S16}$$

$$
\begin{aligned}
u_0 &= \langle S|u(\boldsymbol{r})|S\rangle = \langle X|u(\boldsymbol{r})|X\rangle, \\
\alpha_{ex} &= \langle S|\hat{u}_X(\boldsymbol{r})|S\rangle, \quad \beta_{ex} = \langle X|\hat{u}_X(\boldsymbol{r})|X\rangle.
\end{aligned}
\tag{S17}
$$

Matrix elements of the scattering potential take the form:

$$
\begin{aligned}
V_{kk'}^{ss'} = \langle\chi_s|u_0\left(1 + (\mathcal{A}^2 + 2\mathcal{B}^2)(\boldsymbol{k}\cdot\boldsymbol{k'}) + i(2\mathcal{A}\mathcal{B} + \mathcal{B}^2)\hat{\boldsymbol{\sigma}}\cdot(\boldsymbol{k}\times\boldsymbol{k'})\right) + \alpha_{ex}(\boldsymbol{J}\cdot\hat{\boldsymbol{\sigma}}) + \\
+\beta_{ex}\left(i(2\mathcal{A}\mathcal{B} - \mathcal{B}^2)\boldsymbol{J}\cdot(\boldsymbol{k}\times\boldsymbol{k'}) + \mathcal{A}^2(\boldsymbol{J}\cdot\hat{\boldsymbol{\sigma}})(\boldsymbol{k}\cdot\boldsymbol{k'}) - \mathcal{B}^2(\boldsymbol{J}\cdot\boldsymbol{k})(\hat{\boldsymbol{\sigma}}\cdot\boldsymbol{k'}) - \mathcal{B}^2(\hat{\boldsymbol{\sigma}}\cdot\boldsymbol{k})(\boldsymbol{J}\cdot\boldsymbol{k'})\right)|\chi_{s'}\rangle,
\end{aligned}
\tag{S18}
$$

Some of these terms do not contribute to the the asymmetric scattering and can be omitted resulting in a more compact expression:

$$
V_{kk'}^{ss'} = \langle\chi_s|u_0\left(1 + i(2\mathcal{A}\mathcal{B} + \mathcal{B}^2)\hat{\boldsymbol{\sigma}}\cdot(\boldsymbol{k}\times\boldsymbol{k'})\right) + \alpha_{ex}(\boldsymbol{J}\cdot\hat{\boldsymbol{\sigma}}) + \beta_{ex}\left(i(2\mathcal{A}\mathcal{B} - \mathcal{B}^2)\boldsymbol{J}\cdot(\boldsymbol{k}\times\boldsymbol{k'})\right)|\chi_{s'}\rangle,
\tag{S19}
$$

$$
|V_{kk'}^{ss'}|^2 = u_0^2\delta_{ss'} + 2u_0\alpha_{ex}J\sigma_z^{ss'} + \alpha_{ex}^2 J^2\delta_{ss'} = (u_0 \pm \alpha_{ex}J)^2\delta_{ss'}.
\tag{S20}
$$

Expressions for the skew scattering rate (S1), relaxation time (S4), A and B-matrices (S5) to be further used in Boltzmann kinetic equation, are given below:

$$
\begin{aligned}
W_{kk'}^{ss'} &= -2\pi\nu u_0^2(\boldsymbol{k}\times\boldsymbol{k'})_z(\sigma_z^{ss'}Z_0 + \delta_{ss'}Z_X), \\
Z_0 &= u_0(2\mathcal{A}\mathcal{B} + \mathcal{B}^2), \\
Z_X &= \beta_{ex}J(2\mathcal{A}\mathcal{B} - \mathcal{B}^2) + 2\alpha_{ex}J(2\mathcal{A}\mathcal{B} + \mathcal{B}^2),
\end{aligned}
\tag{S21}
$$

$$
\nu = \frac{mk}{2\pi^2\hbar^2} = \frac{m\sqrt{2m\varepsilon}}{2\pi^2\hbar^3},
\tag{S22}
$$

$$
\frac{1}{\tau_{\uparrow\downarrow}} = \frac{2\pi}{\hbar}n_i\nu(u_0 \pm \alpha_{ex}J)^2,
\tag{S23}
$$

$$
\Delta\tau = \tau_\downarrow - \tau_\uparrow = \frac{4\alpha_{ex}J}{\frac{2\pi}{\hbar}n_i\nu u_0^3},
\tag{S24}
$$

$$
A = \begin{pmatrix} -\frac{1}{\tau_\uparrow} & 0 \\ 0 & -\frac{1}{\tau_\downarrow} \end{pmatrix}, \qquad B = \frac{4\pi^2}{\hbar}n_i\nu^2u_0^2\frac{4\pi}{3}k^2\begin{pmatrix} Z_0 + Z_X & 0 \\ 0 & -Z_0 + Z_X \end{pmatrix}.
\tag{S25}
$$

The Boltzmann kinetic equation then takes the following form:

$$
eE_x\frac{\partial f^0}{\partial\varepsilon}\begin{pmatrix} v \\ v \\ 0 \\ 0 \end{pmatrix} = \begin{pmatrix} A & -B \\ B & A \end{pmatrix}\begin{pmatrix} f_x^\uparrow \\ f_x^\downarrow \\ f_y^\uparrow \\ f_y^\downarrow \end{pmatrix},
\tag{S26}
$$

where f_x, f_y are coefficients in non-equilibrium distribution function expansion in spherical harmonics Y_x, Y_y, Y_z according to equation:

$$
\delta f_s(\boldsymbol{k}) = f_x^s(k)Y_x + f_y^s(k)Y_y + f_z^s(k)Y_z.
\tag{S27}
$$

As B-matrix is of third order in scattering potential (compared to second order of A-matrix), we can neglect it to find coefficients f_x^s, and then use expressions for them to find f_y^s, according to (S9). The solution for these coefficients yields

$$
f_x^s = -eE_x\frac{\partial f^0}{\partial\varepsilon}\tau_s v,
\tag{S28}
$$

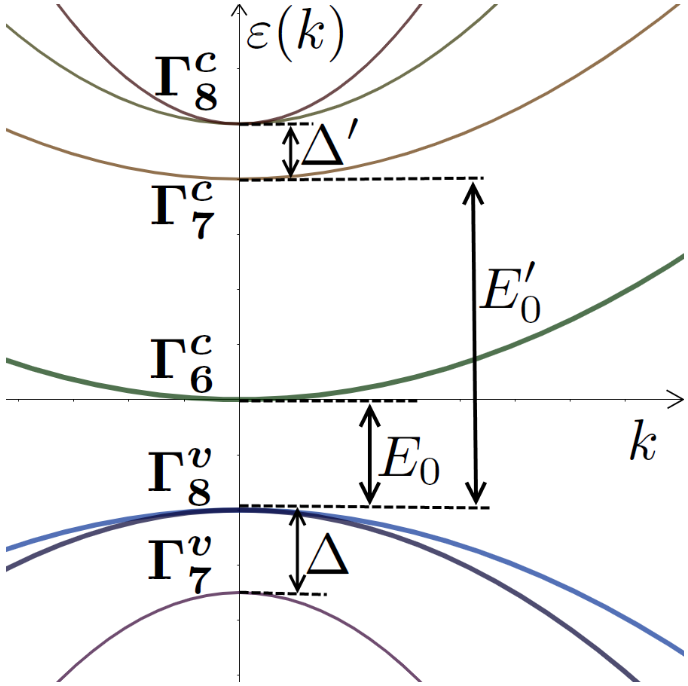

FIG. S1. Band diagram for a semiconductor with zinc-blend crystal structure

$$f_y^s = -eE_x \frac{\partial f^0}{\partial \varepsilon} \frac{8\pi^3 \hbar^2}{m n_i u_0^2} n_s (\pm Z_0 - 4\frac{\alpha_{ex} J}{u_0} Z_0 + Z_X). \tag{S29}$$

We further calculate the transverse Hall current according to (S10). We obtain

$$j_y = \left(P_s \theta_0 - \theta_0 \frac{\Delta \tau}{\tau} + \theta_X \right) \sigma_0 E_x, \tag{S30}$$

where $\theta_{0,X}$ are Hall angles, and P_s is electron spin polarization

$$\theta_{0,X} = Z_{0,X} \frac{2\pi}{3} \nu k_F^2, \quad P_s = \frac{n_\uparrow - n_\downarrow}{n_\uparrow + n_\downarrow}. \tag{S31}$$

B. Valence band

The Γ_8 states of the valence band can be described by Luttinger Hamiltonian

$$H = \frac{\hbar^2}{2m_0} \left((\gamma_1 + \frac{5}{2}\gamma_2) \boldsymbol{k}^2 - 2\gamma_2 (\boldsymbol{k} \cdot \hat{\boldsymbol{\mathcal{J}}})^2 \right), \tag{S32}$$

The eigenfunctions in the canonical basis [S2] take the form. Here we use the form of a fixed helicity, $\pm$ denotes the helicity sign and lh, hh denote light holes and heave holes, respectively:

$$\Psi_{lh,+}(\boldsymbol{k}) = \Psi_{lh,-}(-\boldsymbol{k}) = \begin{pmatrix} -\sqrt{3}\sin\frac{\theta}{2}\cos^2\frac{\theta}{2}e^{-\frac{3i\varphi}{2}} \\ (3\cos^2\frac{\theta}{2}-2)\cos\frac{\theta}{2}e^{-\frac{i\varphi}{2}} \\ -(3\sin^2\frac{\theta}{2}-2)\sin\frac{\theta}{2}e^{\frac{i\varphi}{2}} \\ \sqrt{3}\sin^2\frac{\theta}{2}\cos\frac{\theta}{2}e^{\frac{3i\varphi}{2}} \end{pmatrix}, \tag{S33}$$

$$\Psi_{hh,+}(\boldsymbol{k}) = \Psi_{hh,-}(-\boldsymbol{k}) = \begin{pmatrix} \cos^3\frac{\theta}{2}e^{-\frac{3i\varphi}{2}} \\ \sqrt{3}\sin\frac{\theta}{2}\cos^2\frac{\theta}{2}e^{-\frac{i\varphi}{2}} \\ \sqrt{3}\sin^2\frac{\theta}{2}\cos\frac{\theta}{2}e^{\frac{i\varphi}{2}} \\ \sin^3\frac{\theta}{2}e^{\frac{3i\varphi}{2}} \end{pmatrix}. \tag{S34}$$

Let us further account for the admixture of other bands in the leading order in $k.p$: For lh the admixture of Γ_6 leads to the following corrections to the wavefunctions

$$\delta\Psi_{lh,+} = \frac{ikP}{E_0}\frac{\sqrt{6}}{3}\cos\frac{\theta}{2}e^{-\frac{i\varphi}{2}}|S\uparrow\rangle + \frac{ikP}{E_0}\frac{\sqrt{6}}{3}\sin\frac{\theta}{2}e^{\frac{i\varphi}{2}}|S\downarrow\rangle, \tag{S35}$$

$$\delta\Psi_{lh,-} = \frac{ikP}{E_0}\frac{\sqrt{6}i}{3}\sin\frac{\theta}{2}e^{-\frac{i\varphi}{2}}|S\uparrow\rangle - \frac{ikP}{E_0}\frac{\sqrt{6}i}{3}\cos\frac{\theta}{2}e^{\frac{i\varphi}{2}}|S\downarrow\rangle, \tag{S36}$$

$$\delta\Psi_{hh,+} = \delta\Psi_{hh,-} = 0. \tag{S37}$$

For hh the admixture of Γ_7^c, Γ_8^c results in the following corrections to the wavefunctions. Here we neglect the correction due to non-diagonal matrix element Δ^- of the SOC term between the Γ^8 and Γ_8^c, as it does not contribute to the final result.

$$\begin{aligned} \delta\Psi_{lh,+} = &\frac{ikQ}{E_0'+\Delta'}\left(\frac{i\sqrt{3}}{3}e^{-\frac{3i}{2}\varphi}\sin\frac{\theta}{2}\cos^2\frac{\theta}{2}\right)|1'\rangle + \\ &+\frac{ikQ}{E_0'+\Delta'}\left(-ie^{-\frac{i\varphi}{2}}\cos^3\frac{\theta}{2}+\frac{2i}{3}e^{-\frac{i\varphi}{2}}\cos\frac{\theta}{2}\right)|2'\rangle + \\ &+\frac{ikQ}{E_0'+\Delta'}\left(ie^{\frac{i\varphi}{2}}\sin^3\frac{\theta}{2}-\frac{2i}{3}e^{\frac{i\varphi}{2}}\sin\frac{\theta}{2}\right)|3'\rangle + \\ &+\frac{ikQ}{E_0'+\Delta'}\left(-\frac{\sqrt{3}i}{3}e^{\frac{3i}{2}\varphi}\cos\frac{\theta}{2}\sin^2\frac{\theta}{2}\right)|4'\rangle + \\ &+\frac{ikQ}{E_0'}\left(-\frac{\sqrt{2}i}{3}e^{-\frac{i\varphi}{2}}\cos\frac{\theta}{2}\right)|5'\rangle + \\ &+\frac{ikQ}{E_0'}\left(-\frac{\sqrt{2}i}{3}e^{\frac{i\varphi}{2}}\sin\frac{\theta}{2}\right)|6'\rangle \end{aligned} \quad \begin{aligned} \delta\Psi_{lh,-} = &\frac{ikQ}{E_0'+\Delta'}\left(\frac{\sqrt{3}}{3}e^{-\frac{3i}{2}\varphi}\sin^2\frac{\theta}{2}\cos\frac{\theta}{2}\right)|1'\rangle + \\ &+\frac{ikQ}{E_0'+\Delta'}\left(e^{-\frac{i\varphi}{2}}\sin^3\frac{\theta}{2}-\frac{2}{3}e^{-\frac{i\varphi}{2}}\sin\frac{\theta}{2}\right)|2'\rangle + \\ &+\frac{ikQ}{E_0'+\Delta'}\left(e^{\frac{i\varphi}{2}}\cos^3\frac{\theta}{2}-\frac{2}{3}e^{\frac{i\varphi}{2}}\cos\frac{\theta}{2}\right)|3'\rangle + \\ &+\frac{ikQ}{E_0'+\Delta'}\left(\frac{\sqrt{3}}{3}e^{\frac{3i}{2}\varphi}\sin\frac{\theta}{2}\cos^2\frac{\theta}{2}\right)|4'\rangle + \\ &+\frac{ikQ}{E_0'}\left(\frac{\sqrt{2}}{3}e^{-\frac{i\varphi}{2}}\sin\frac{\theta}{2}\right)|5'\rangle + \\ &+\frac{ikQ}{E_0'}\left(-\frac{\sqrt{2}}{3}e^{\frac{i\varphi}{2}}\cos\frac{\theta}{2}\right)|6'\rangle \end{aligned} \tag{S38}$$

$$\begin{aligned} \delta\Psi_{hh,+} = &\frac{ikQ}{E_0'+\Delta'}\left(-ie^{-\frac{3i}{2}\varphi}\cos^3\frac{\theta}{2}\right)|1'\rangle + \\ &+\frac{ikQ}{E_0'+\Delta'}\left(-\sqrt{3}ie^{-\frac{i\varphi}{2}}\sin\frac{\theta}{2}\cos^2\frac{\theta}{2}\right)|2'\rangle + \\ &+\frac{ikQ}{E_0'+\Delta'}\left(-\sqrt{3}ie^{\frac{i\varphi}{2}}\sin^2\frac{\theta}{2}\cos\frac{\theta}{2}\right)|3'\rangle + \\ &+\frac{ikQ}{E_0'+\Delta'}\left(-ie^{\frac{3i}{2}\varphi}\sin^3\frac{\theta}{2}\right)|4'\rangle + \end{aligned} \quad \begin{aligned} \delta\Psi_{hh,-} = &\frac{ikQ}{E_0'+\Delta'}\left(-e^{-\frac{3i}{2}\varphi}\sin^3\frac{\theta}{2}\right)|1'\rangle + \\ &+\frac{ikQ}{E_0'+\Delta'}\left(\sqrt{3}e^{-\frac{i\varphi}{2}}\sin^2\frac{\theta}{2}\cos\frac{\theta}{2}\right)|2'\rangle + \\ &+\frac{ikQ}{E_0'+\Delta'}\left(-\sqrt{3}e^{\frac{i\varphi}{2}}\sin\frac{\theta}{2}\cos^2\frac{\theta}{2}\right)|3'\rangle + \\ &+\frac{ikQ}{E_0'+\Delta'}\left(e^{\frac{3i}{2}\varphi}\cos^3\frac{\theta}{2}\right)|4'\rangle + \end{aligned} \tag{S39}$$

where $1', 2', 3', 4'$ denote the canonical basis of the upper band at Γ-point, and

$$Q = \frac{i\hbar}{m}\langle X'|\hat{p}_y|Z\rangle. \tag{S40}$$

The contribution due to Δ^- matrix element:

$$\Delta^- = 3\langle 1'|H_{so}|1\rangle = 3\langle 2'|H_{so}|2\rangle = 3\langle 3'|H_{so}|3\rangle = 3\langle 4'|H_{so}|4\rangle, \quad H_{SO} = \frac{1}{4m_0^2c^2}\hat{\boldsymbol{p}}\cdot(\hat{\boldsymbol{\sigma}}\times\nabla V(\boldsymbol{r}))\,, \tag{S41}$$

$$\delta\Psi^{(1)}_{lh,+} = \frac{\sqrt{3}\Delta^- e^{-i\varphi}\sin 2\theta}{6E_0'\sqrt{1+3\cos^2\theta}}|1'\rangle - \frac{\Delta^-}{6E_0'}\sqrt{1+3\cos^2\theta}|2'\rangle + \frac{\sqrt{3}\Delta^- e^{2i\varphi}\sin^2\theta}{6E_0'\sqrt{1+3\cos^2\theta}}|4'\rangle, \tag{S42}$$

$$\delta\Psi^{(1)}_{lh,-} = \frac{\sqrt{3}\Delta^- e^{-2i\varphi}\sin^2\theta}{6E_0'\sqrt{1+3\cos^2\theta}}|1'\rangle - \frac{\Delta^-}{6E_0'}\sqrt{1+3\cos^2\theta}|3'\rangle - \frac{\sqrt{3}\Delta^- e^{i\varphi}\sin 2\theta}{6E_0'\sqrt{1+3\cos^2\theta}}|4'\rangle, \tag{S43}$$

$$\delta\Psi^{(1)}_{hh,+} = \frac{\Delta^- e^{-i\varphi}\sin 2\theta}{6E_0'\sin\theta}|1'\rangle + \frac{\sqrt{3}\Delta^-}{6E_0'}\sin\theta|2'\rangle + \frac{\Delta^-}{6E_0'}e^{2i\varphi}\sin\theta|4'\rangle, \tag{S44}$$

$$\delta\Psi^{(1)}_{hh,-} = \frac{\Delta^-}{6E_0'}e^{-2i\varphi}\sin\theta|1'\rangle + \frac{\sqrt{3}\Delta^-}{6E_0'}\sin\theta|3'\rangle - \frac{\Delta^- e^{i\varphi}\sin 2\theta}{6E_0'\sin\theta}|4'\rangle. \tag{S45}$$

First spherical harmonics are defined as:

$$Y_x = \sqrt{\frac{3}{4\pi}}\sin\theta\cos\varphi, \qquad Y_y = \sqrt{\frac{3}{4\pi}}\sin\theta\sin\varphi, \qquad Y_z = \sqrt{\frac{3}{4\pi}}\cos\theta. \tag{S46}$$

The first spherical harmonics of the scattering rates for different cases are presented below (for simplicity we tase $u_0 = 1$). For Lattinger hamiltonian:

$$\begin{aligned} W^{(1)}_{lh+,lh+} = -W^{(1)}_{lh+,lh-} = W^{(1)}_{lh-,lh-} &= \frac{\pi^2}{15}\langle\nu\rangle\beta_{ex}(Y_x'Y_y - Y_y'Y_x), \\ W^{(1)}_{lh+,hh+} = -W^{(1)}_{lh+,hh-} = -W^{(1)}_{lh-,hh+} = W^{(1)}_{lh-,hh-} &= \frac{\pi^2}{5}\langle\nu\rangle\beta_{ex}(Y_x'Y_y - Y_y'Y_x), \\ W^{(1)}_{hh+,hh+} = -W^{(1)}_{hh+,hh-} = W^{(1)}_{hh-,hh-} &= \frac{3\pi^2}{5}\langle\nu\rangle\beta_{ex}(Y_x'Y_y - Y_y'Y_x), \end{aligned} \tag{S47}$$

$$\frac{1}{\tau_{lh\pm}} = \frac{1}{\tau_{hh\pm}} = \frac{8\pi^2}{\hbar}n_i\langle\nu\rangle, \tag{S48}$$

where $\langle\nu\rangle = (\nu_{lh} + \nu_{hh})/2$,

$$\left(|V_{lh+,lh+}|^2\right)^{(1)} = -\left(|V_{lh+,lh-}|^2\right)^{(1)} = \left(|V_{lh-,lh-}|^2\right)^{(1)} = \frac{\pi}{15}(Y_xY_x' + Y_yY_y' + Y_zY_z'), \tag{S49}$$

$$\left(|V_{lh+,hh+}|^2\right)^{(1)} = -\left(|V_{lh+,hh-}|^2\right)^{(1)} = -\left(|V_{lh-,hh+}|^2\right)^{(1)} = \left(|V_{lh-,hh-}|^2\right)^{(1)} = \frac{\pi}{5}(Y_xY_x' + Y_yY_y' + Y_zY_z'), \tag{S50}$$

$$\left(|V_{hh+,hh+}|^2\right)^{(1)} = -\left(|V_{hh+,hh-}|^2\right)^{(1)} = \left(|V_{lh-,lh-}|^2\right)^{(1)} = \frac{3\pi}{5}(Y_xY_x' + Y_yY_y' + Y_zY_z'). \tag{S51}$$

With admixture of Γ_6 band.

$$W^{(1)}_{lh+,lh+} = W^{(1)}_{lh+,lh-} = W^{(1)}_{lh-,lh-} = \frac{2\pi^2\langle\nu\rangle kk'P^2}{9E_0^2}(\alpha_{ex} + 10\beta_{ex}), \tag{S52}$$

$$\frac{1}{\tau_{lh\pm}} = \frac{8\pi^2}{\hbar} n_i \langle\nu\rangle + \frac{32\pi^2 \nu_{lh} (kk')^2 P^4}{9\hbar E_0^4} n_i, \tag{S53}$$

$$\left(|V_{lh+,lh+}|^2\right)^{(1)} = \left(|V_{lh-,lh-}|^2\right)^{(1)} = \left(\frac{\pi}{15} + \frac{8\pi}{9}\frac{P^2}{E_0^2} kk' + \frac{8\pi}{27}\frac{P^4}{E_0^4}(kk')^2\right)(Y_x Y'_x + Y_y Y'_y + Y_z Y'_z), \tag{S54}$$

$$\left(|V_{lh+,lh-}|^2\right)^{(1)} = \left(-\frac{\pi}{15} + \frac{8\pi}{9}\frac{P^2}{E_0^2} kk' - \frac{8\pi}{27}\frac{P^4}{E_0^4}(kk')^2\right)(Y_x Y'_x + Y_y Y'_y + Y_z Y'_z). \tag{S55}$$

The resulting transverse electric current is

$$j_y = \frac{\hbar}{2\pi n_i} e^2 E_x (\nu_{lh} v_{lh} k_{lh})^2 \frac{\left(\frac{P}{E_0}\right)^2 (\alpha_{ex} + 10\beta_{ex})}{18\langle\nu\rangle u_0^2}. \tag{S56}$$

With admixture of $\Gamma^c_{7,8}$:

$$\begin{aligned} W^{(1)}_{lh+,lh+} = W^{(1)}_{lh-,lh-} = W^{(1)}_{lh+,lh-} = \Bigg(\frac{2}{9}\pi^2 \left(\frac{P}{E_0}\right)^2 \langle\nu\rangle k_{lh}^2 (\alpha_{ex} + 10\beta_{ex}) + \\ + \frac{\langle\nu\rangle}{135}\pi^2 \left(\frac{Q}{E'_0 + \Delta'}\right)^2 k_{lh}^2 (2\beta_{ex} - \gamma_{ex}) + \frac{2}{27}\pi^2 \left(\frac{Q}{E'_0}\right)^2 \langle\nu\rangle k_{lh}^2 (10\beta_{ex} + \gamma_{ex})\Bigg)(Y'_x Y_y - Y'_y Y_x), \end{aligned} \tag{S57}$$

$$W^{(1)}_{lh+,hh+} = W^{(1)}_{lh-,hh-} = W^{(1)}_{lh+,hh-} = W^{(1)}_{lh-,hh+} = \left(\frac{\langle\nu\rangle}{15}\pi^2 \left(\frac{Q}{E'_0 + \Delta'}\right)^2 k_{hh} k_{lh} (2\beta_{ex} - \gamma_{ex})\right)(Y'_x Y_y - Y'_y Y_x), \tag{S58}$$

$$W^{(1)}_{hh+,hh+} = W^{(1)}_{hh-,hh-} = W^{(1)}_{hh+,hh-} = \left(\frac{3}{5}\pi^2 \left(\frac{Q}{E'_0 + \Delta'}\right)^2 \langle\nu\rangle k_{hh}^2 (2\beta_{ex} - \gamma_{ex})\right)(Y'_x Y_y - Y'_y Y_x), \tag{S59}$$

$$\begin{aligned} \frac{1}{\tau_{lh\pm}}\frac{\hbar}{2\pi n_i} = \frac{16\pi}{9}\left(\frac{P}{E_0}\right)^4 \nu_{lh} k_{lh}^4 + \frac{32\pi}{27}\left(\frac{P}{E_0}\right)^2 \left(\frac{Q}{E'_0}\right)^2 \nu_{lh} k_{lh}^4 + \\ + \left(\frac{Q}{E'_0 + \Delta'}\right)^4 \left(\frac{4\pi}{9}\langle\nu\rangle k_{hh}^2 k_{lh}^2 - \frac{2\pi}{9}\nu_{lh} k_{hh}^2 k_{lh}^2 + \frac{2\pi}{81}\nu_{lh} k_{lh}^4\right) + \frac{16\pi}{81}\left(\frac{Q}{E'_0}\right)^4 \nu_{lh} k_{lh}^4 + 4\pi\langle\nu\rangle, \end{aligned} \tag{S60}$$

$$\frac{1}{\tau_{hh\pm}}\frac{\hbar}{2\pi n_i} = \left(\frac{Q}{E'_0 + \Delta'}\right)^4 \left(4\pi\langle\nu\rangle k_{hh}^4 - 2\pi\nu_{lh} k_{hh}^4 + \frac{2\pi}{9}\nu_{lh} k_{hh}^2 k_{lh}^2\right) + 4\pi\langle\nu\rangle, \tag{S61}$$

$$\begin{aligned} &(|V_{lh+,lh+}|^2)^{(1)} = (|V_{lh-,lh-}|^2)^{(1)} = \\ &= \frac{\pi}{15} + \frac{8\pi}{27}\left(\frac{P}{E_0}\right)^4 k_{lh}^4 + \left(\frac{P}{E_0}\right)^2 \left(\frac{8\pi}{81}\left(\frac{Q}{E'_0 + \Delta'}\right)^2 k_{lh}^4 + \frac{16\pi}{81}\left(\frac{Q}{E'_0}\right)^2 k_{lh}^4 + \frac{8\pi}{9} k_{lh}^2\right) + \\ &+ \frac{\pi}{1215}\left(\frac{Q}{E'_0 + \Delta'}\right)^4 k_{lh}^4 + \left(\frac{Q}{E'_0 + \Delta'}\right)^2 \left(\frac{8\pi}{243}\left(\frac{Q}{E'_0}\right)^2 k_{lh}^4 + \frac{2\pi}{135} k_{lh}^2\right) + \frac{8\pi}{243}\left(\frac{Q}{E'_0}\right)^4 k_{lh}^4 + \frac{8\pi}{27}\left(\frac{Q}{E'_0}\right)^2 k_{lh}^2, \end{aligned} \tag{S62}$$

$$\begin{aligned} &(|V_{lh+,lh-}|^2)^{(1)} = \\ &= -\frac{\pi}{15} - \frac{8\pi}{27}\left(\frac{P}{E_0}\right)^4 k_{lh}^4 + \left(\frac{P}{E_0}\right)^2 \left(-\frac{8\pi}{81}\left(\frac{Q}{E'_0 + \Delta'}\right)^2 k_{lh}^4 - \frac{16\pi}{81}\left(\frac{Q}{E'_0}\right)^2 k_{lh}^4 + \frac{8\pi}{9} k_{lh}^2\right) + \\ &- \frac{\pi}{1215}\left(\frac{Q}{E'_0 + \Delta'}\right)^4 k_{lh}^4 + \left(\frac{Q}{E'_0 + \Delta'}\right)^2 \left(-\frac{8\pi}{243}\left(\frac{Q}{E'_0}\right)^2 k_{lh}^4 + \frac{2\pi}{135} k_{lh}^2\right) - \frac{8\pi}{243}\left(\frac{Q}{E'_0}\right)^4 k_{lh}^4 + \frac{8\pi}{27}\left(\frac{Q}{E'_0}\right)^2 k_{lh}^2, \end{aligned} \tag{S63}$$

$$(|V_{lh+,hh+}|^2)^{(1)} = (|V_{lh-,hh-}|^2)^{(1)} = \frac{\pi}{45}\left(\frac{Q}{E_0'+\Delta'}\right)^4 k_{hh}^2 k_{lh}^2 + \frac{2\pi}{15}\left(\frac{Q}{E_0'+\Delta'}\right)^2 k_{hh}k_{lh} + \frac{\pi}{5}, \tag{S64}$$

$$(|V_{lh+,hh-}|^2)^{(1)} = (|V_{lh-,hh+}|^2)^{(1)} = -\frac{\pi}{45}\left(\frac{Q}{E_0'+\Delta'}\right)^4 k_{hh}^2 k_{lh}^2 + \frac{2\pi}{15}\left(\frac{Q}{E_0'+\Delta'}\right)^2 k_{hh}k_{lh} - \frac{\pi}{5}, \tag{S65}$$

$$(|V_{hh+,hh+}|^2)^{(1)} = (|V_{hh-,hh-}|^2)^{(1)} = \frac{3\pi}{5}\left(\frac{Q}{E_0'+\Delta'}\right)^4 k_{hh}^4 + \frac{6\pi}{5}\left(\frac{Q}{E_0'+\Delta'}\right)^2 k_{hh}^2 + \frac{3\pi}{5}, \tag{S66}$$

$$(|V_{hh+,hh-}|^2)^{(1)} = -\frac{3\pi}{5}\left(\frac{Q}{E_0'+\Delta'}\right)^4 k_{hh}^4 + \frac{6\pi}{5}\left(\frac{Q}{E_0'+\Delta'}\right)^2 k_{hh}^2 - \frac{3\pi}{5}. \tag{S67}$$

Using equation (S10), we obtain:

$$\begin{aligned} j_y^{lh} = 2e^2 E_x \nu_{lh} v_{lh} \Bigg(&\left(\frac{P}{E_0}\right)^2 \frac{\nu_{lh} v_{lh}}{36\langle\nu\rangle} k_{lh}^2 \left(\alpha_{ex} + 10\beta_{ex}\right) + \\ &+ \left(\frac{Q}{E_0'+\Delta'}\right)^2 \frac{k_{lh}}{1080\langle\nu\rangle} \left(2\beta_{ex} - \gamma_{ex}\right) \left(9\nu_{hh} k_{hh} v_{hh} + \nu_{lh} k_{lh} v_{lh}\right) + \\ &+ \left(\frac{Q}{E_0'}\right)^2 \frac{\nu_{lh} v_{lh}}{108\langle\nu\rangle} k_{lh}^2 \left(10\beta_{ex} + \gamma_{ex}\right) \Bigg), \end{aligned} \tag{S68}$$

$$j_y^{hh} = 2e^2 E_x \nu_{hh} v_{hh} \left(\frac{Q}{E_0'+\Delta'}\right)^2 \frac{k_{hh}}{120\langle\nu\rangle} \left(2\beta_{ex} - \gamma_{ex}\right) \left(9\nu_{hh} k_{hh} v_{hh} + \nu_{lh} k_{lh} v_{lh}\right). \tag{S69}$$

III. SPIN CURRENT

A. Solving Boltzmann kinetic equation with higher harmonics taken into account.

We start with the Boltzmann kinetic equation

$$(e\boldsymbol{E}\boldsymbol{v}_s)\frac{\partial f_s^0}{\partial \varepsilon} = \mathrm{St}[\delta f_s] \tag{S70}$$

with collision integral split into two terms

$$\begin{aligned} \mathrm{St}_1[\delta f_s(\boldsymbol{k})] &= \frac{2\pi}{\hbar} n_i \sum_{s'\boldsymbol{k'}} \delta(\varepsilon_k^s - \varepsilon_{k'}^{s'}) |V_{kk'}^{ss'}|^2 \delta f_{s'}(\boldsymbol{k'}) - \frac{\delta f_s(\boldsymbol{k})}{\tau_s}, \\ \mathrm{St}_2[\delta f_s(\boldsymbol{k})] &= \frac{2\pi}{\hbar} n_i \sum_{s'\boldsymbol{k'}} \delta(\varepsilon_k^s - \varepsilon_{k'}^{s'}) W_{kk'}^{ss'} \delta f_{s'}(\boldsymbol{k'}). \end{aligned} \tag{S71}$$

Since both $|V_{kk'}^{ss'}|^2$ and $W_{kk'}^{ss'}$ might depend on $\boldsymbol{k}$ and $\boldsymbol{k'}$ wavevectors' directions in a complicated way, an approach using only first spherical harmonics (S2) seems to be naive. However, a more complicated calculation with a complete spherical harmonics decomposition leads to the same result. This calculation is presented below.

We present direction dependent quantities as a sum over spherical harmonics $Y_n(\frac{\boldsymbol{k}}{|k|})$, $Y'_{n'}(\frac{\boldsymbol{k'}}{|k'|})$, where n and n' are pairs of indexes $n = (l, m)$, $n' = (l', m')$.

$$|V_{kk'}^{ss'}|^2 = \sum_{nn'} v_{nn'}^{ss'} Y_n Y'_{n'}, \tag{S72}$$

$$W_{kk'}^{ss'} = \sum_{nn'} w_{nn'}^{ss'} Y_n Y'_{n'}, \tag{S73}$$

$$\delta f_s(\Omega) = \sum_n f_n^s Y_n. \tag{S74}$$

With this representation, the first term in the collision integral (S71) can be transformed as follows:

$$\mathrm{St}_1[\delta f_s(\boldsymbol{k})] = \frac{2\pi}{\hbar} n_i \sum_{s'} \nu_{s'} \frac{1}{4\pi} \left(\sum_{nn'} v_{nn'}^{ss'} f_{n'}^{s'} Y_n - \sqrt{4\pi} \sum_{nmn'} v_{n0}^{ss'} f_m^s K_{n'nm} Y_{n'} \right), \tag{S75}$$

where $K_{n'nm} = \int \mathrm{d}\,\Omega Y_{n'} Y_n Y_m$ can be expressed in terms of Clebsch-Gordan coefficients. Since there is no direction independent terms in the expression for $W_{kk'}^{ss'}$, i.e. $\langle W_{kk'}^{ss'} \rangle_{\Omega'} = 0$, the second part of the integral collisions is converted as

$$\mathrm{St}_2[\delta f_s(\boldsymbol{k})] = \frac{2\pi}{\hbar} n_i \sum_{s'} \nu_{s'} \frac{1}{4\pi} \sum_{nn'} w_{nn'}^{ss'} f_{n'}^{s'} Y_n. \tag{S76}$$

Then we need to multiply both sides of the kinetic equation by Y_n and take an average over wavevector $\boldsymbol{k}$ direction. This allows us to introduce matrices $A_{nn'}^{ss'}$, $B_{nn'}^{ss'}$ and F_n^s, so that the kinetic equation can be presented in a matrix form.

$$\langle Y_n \, \mathrm{St}_1[\delta f_s(\boldsymbol{k})] \rangle_\Omega = \sum_{s'n'} \underbrace{\frac{2\pi}{\hbar} n_i \frac{1}{(4\pi)^2} \left(\nu_{s'} v_{nn'}^{ss'} - \sqrt{4\pi} \delta_{ss'} \sum_{s''m} \nu_{s''} v_{m0}^{s's''} K_{nmn'} \right)}_{A_{nn'}^{ss'}} f_{n'}^{s'}, \tag{S77}$$

$$\langle Y_n \, \mathrm{St}_2[\delta f_s(\boldsymbol{k})] \rangle_\Omega = \sum_{s'n'} \underbrace{\frac{2\pi}{\hbar} n_i \frac{1}{(4\pi)^2} \nu_{s'} w_{nn'}^{ss'}}_{B_{nn'}^{ss'}} f_{n'}^{s'}, \tag{S78}$$

$$F_n^s = \langle Y_n e E_x v_x^s \frac{\partial f_s^0(\boldsymbol{k})}{\partial \varepsilon} \rangle_\Omega = \begin{cases} \frac{1}{4\pi} e E_x v_s \frac{\partial f_s^0}{\partial \varepsilon}, & n = (1,1) \\ 0, & n \neq (1,1). \end{cases} \tag{S79}$$

Now we can write the kinetic equation as follows:

$$F_n^s = \sum_{s'n'} A_{nn'}^{ss'} f_{n'}^{s'} + \sum_{s'n'} B_{nn'}^{ss'} f_{n'}^{s'} \tag{S80}$$

or, leaving out matrix indices:

$$F = (A + B) f. \tag{S81}$$

Treating B as a small quantity compared to A, the solution can be presented as

$$f = A^{-1} F - A^{-1} B A^{-1} F. \tag{S82}$$

Matrix A has a rather complicated form, however, it simplifies significantly in the absence of exchange $\varepsilon = 0$. Expanding A into $A_0 = A|_{\varepsilon=0}$ and the addition $\delta A \sim \varepsilon$, we can simplify (S82) a little further.

$$f = A_0^{-1} F - A_0^{-1} \delta A A_0^{-1} F - A_0^{-1} B A_0^{-1} F. \tag{S83}$$

A transverse current appears from the f_y^s coefficients, that is, from the $n = (1,-1)$ harmonic, so the expression above take the following form:

$$f_{1,-1} = -(A_0^{-1})_{(1,-1),(1,-1)} \delta A_{(1,-1),(1,1)} (A_0^{-1})_{(1,1),(1,1)} F_{1,1} - (A_0^{-1})_{(1,-1),(1,-1)} B_{(1,-1),(1,1)} (A_0^{-1})_{(1,1),(1,1)} F_{1,1}. \tag{S84}$$

The first term will vanish after summing over subbands, so the resulting expression for $f_{1,-1}$ is equal to (S9), which ignores presence of higher harmonics.

IV. SCATTERING CROSS-SECTION SIMULATION FOR RASHBA ELECTRONS

A. Scattering framework

In this section we present the results for the numerical evaluation of the electron scattering cross-sections described by the parabolic two-dimensional spectrum with the Rashba spin-orbit coupling (see Eq. from the main text), described by the Hamiltonian:

$$H = \frac{p^2}{2m_*} + \lambda\left(\sigma_x p_y - \sigma_y p_x\right) - h\sigma_z. \tag{S85}$$

Here we also introduced h for a possible Zeeman spin splitting at $k = 0$. The energy spectrum is $\varepsilon_{1,2} = p^2/2m_* \pm \sqrt{h^2 + (\lambda p)^2}$. The asymptotic form of an electron wave-function Ψ with energy E contains an incident plane wave contribution and a divergent cylindrical scattering wave

$$\Psi(r,\theta) = \alpha\psi_1(p_1, E) + \beta\psi_2(p_2, E) + \Psi_1^{sc} + \Psi_2^{sc}$$
$$\psi_{1,2} = e^{ik_{1,2}x}\begin{pmatrix} a_{1,2}(E) \\ -ib_{1,2}(E)\end{pmatrix}, \qquad \Psi_1^{sc} = \frac{e^{ik_1 r}}{\sqrt{-ir}}\begin{pmatrix} a_1(E) \\ -ib_1(E)e^{i\theta}\end{pmatrix}\left[\alpha f_{11} + \beta f_{12}\right], \qquad \Psi_2^{sc} = \frac{e^{ik_2 r}}{\sqrt{-ir}}\begin{pmatrix} a_2(E) \\ -ib_2(E)e^{i\theta}\end{pmatrix}\left[\alpha f_{21} + \beta f_{22}\right], \tag{S86}$$

here α, β describe the initial polarization ($|\alpha|^2 + |\beta|^2 = 1$), θ is the polar angle, which is also the scattering angle, the momenta $p_{1,2}(E)$ for the two spin branches at the fixed energy E are

$$p_{1,2}^2(E) = 2mE + 2m^2\lambda^2 \pm 2m^2\sqrt{\lambda^2 2E/m + \lambda^4 + h^2/m^2}, \tag{S87}$$

and the spinors are given by

$$a_i(E) = \frac{\lambda p_i}{\sqrt{(\lambda p_i)^2 + (\mu h + E - p_i^2/2m_*)^2}}, \qquad b_i(E) = \frac{\mu h + E - p_i^2/2m_*}{\sqrt{(\lambda p_i)^2 + (\mu h + E - p_i^2/2m_*)^2}}. \tag{S88}$$

We also consider $E > h$, when two spin branches are allowed for the electron motion. The four elements f_{ij} constitute the matrix of the scattering amplitudes. For the incident flux normalized to the group velocity in the initial subband $v_i = \partial\varepsilon_i/\partial p$ the scattering cross-section can be presented as

$$\sigma_{ij}(\theta) = \frac{v_i}{v_j}|f_{ij}(\theta)|^2 \tag{S89}$$

To analyze the scattering within different scattering channels one thus needs to calculate f_{ij}.

B. Phase function method

To calculate numerically f_{ij} we use the so-called phase function method, described in details in . Namely, for the Rashba ferromagnet Hamiltonian the total wavefunction Ψ can be expanded in a series over angular harmonics

$$\psi_m^i = e^{im\theta}\begin{pmatrix} a_i(E)Z_m(k_i r) \\ b_i(E)Z_{m+1}(k_i r)e^{i\theta}\end{pmatrix},$$

where $Z_m = (J_m, Y_m)$ corresponds to m-th Bessel's function. With this in mind the matrix f_{ij} can be also presented as a sum

$$f = \frac{1}{i\sqrt{2\pi k_1}}\sum_m e^{im\theta}\begin{pmatrix} (S_m^{11} - 1) & S_m^{12} \\ \sqrt{\frac{k_1}{k_2}}S_m^{21} & \sqrt{\frac{k_1}{k_2}}(S_m^{22} - 1)\end{pmatrix},$$
$$S_m = (1 + iK_m)(1 - iK_m)^{-1} \qquad K_m = \begin{pmatrix} \tan\delta_m^1 & t_m^{12} \\ t_m^{21} & \tan\delta_m^2\end{pmatrix},$$

where $\delta_m^{1,2}$ are the scattering phases for m-harmonics and $t_m^{1,2}$ are the mixing parameters.

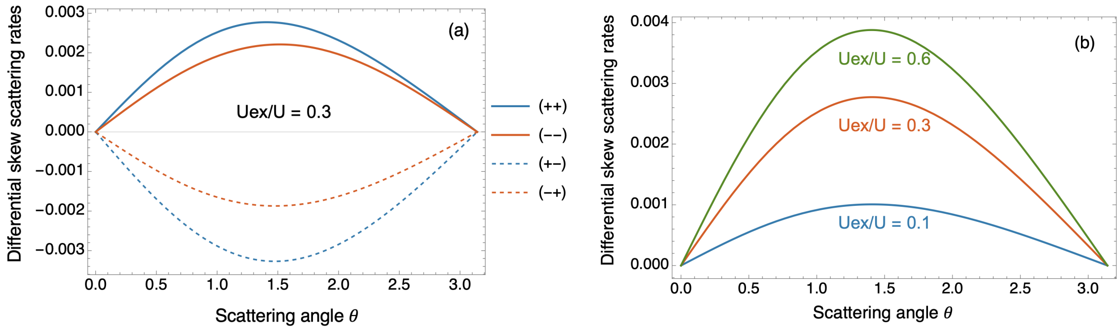

FIG. S2. Asymmetric part of the scattering cross-section calculated numerically via the phase function method. The parameters $m_*\lambda^2/E = 0.16$, $\sqrt{2m_*E}R_0/\hbar = 0.6$. Panel (a): Asymmetric part of the scattering cross-section for different scattering channels. Panel (b): Asymmetric part of the scattering cross-section for the $(++)$ scattering channel at different u_{ex}/u_0.

The key idea of the phase function method is to replace the second order Schrodinger equation by the first order Cauchy problem on the so-called phase functions. We present the contribution Ψ_m of m-th harmonic to the total wavefunction in the following form (after the cancellation of angular factors)

$$\Psi_m = A_1(r)\begin{pmatrix} a_1 J_m(k_1 r) \\ b_1 J_{m+1}(k_1 r)\end{pmatrix} + A_2(r)\begin{pmatrix} a_2 J_m(k_2 r) \\ b_2 J_{m+1}(k_2 r)\end{pmatrix} + A_3(r)\begin{pmatrix} a_1 Y_m(k_1 r) \\ b_1 Y_{m+1}(k_1 r)\end{pmatrix} + A_4(r)\begin{pmatrix} a_2 Y_m(k_2 r) \\ b_2 Y_{m+1}(k_2 r)\end{pmatrix}, \tag{S90}$$

and demand the following condition for the phase functions $A_n(r)$

$$0 = A_1'(r)\begin{pmatrix} a_1 J_m(k_1 r) \\ b_1 J_{m+1}(k_1 r)\end{pmatrix} + A_2'(r)\begin{pmatrix} a_2 J_m(k_2 r) \\ b_2 J_{m+1}(k_2 r)\end{pmatrix} + A_3'(r)\begin{pmatrix} a_1 Y_m(k_1 r) \\ b_1 Y_{m+1}(k_1 r)\end{pmatrix} + A_4'(r)\begin{pmatrix} a_2 Y_m(k_2 r) \\ b_2 Y_{m+1}(k_2 r)\end{pmatrix}. \tag{S91}$$

Using the second relation and simplifying the Schrodinger equation we get the system of first order differential equations on $\vec{A} = \{A_1, A_2, A_3, A_4\}$ function merely

$$\frac{d}{dr}\vec{A} = (\hat{M}^{-1}\cdot\hat{V})\vec{A}, \tag{S92}$$

where the matrix $\hat{M}$ is given by

$$\hat{M} = \begin{pmatrix} a_1 J_m'(k_1 r) & a_2 J_m'(k_2 r) & a_1 Y_m'(k_1 r) & a_2 Y_m'(k_2 r) \\ b_1 J_{m+1}'(k_1 r) & b_2 J_{m+1}'(k_2 r) & b_1 Y_{m+1}'(k_1 r) & b_2 Y_{m+1}'(k_2 r) \\ a_1 J_m(k_1 r) & a_2 J_m(k_2 r) & a_1 Y_m(k_1 r) & a_2 Y_m(k_2 r) \\ b_1 J_{m+1}(k_1 r) & b_2 J_{m+1}(k_2 r) & b_1 Y_{m+1}(k_1 r) & b_2 Y_{m+1}(k_2 r)\end{pmatrix} \tag{S93}$$

and $\hat{V}$ stems from the scattering potential

$$\hat{V} = \begin{pmatrix} (u_0+J_z)a_1 J_m(k_1 r) & (u_0+J_z)a_2 J_m(k_2 r) & (u_0+J_z)a_1 Y_m(k_1 r) & (u_0+J_z)a_2 Y_m(k_2 r) \\ (u_0-J_z)b_1 J_{m+1}(k_1 r) & (u_0-J_z)b_2 J_{m+1}(k_2 r) & (u_0-J_z)b_1 Y_{m+1}(k_1 r) & (u_0-J_z)b_2 Y_{m+1}(k_2 r) \\ 0 & 0 & 0 & 0 \\ 0 & 0 & 0 & 0\end{pmatrix}, \tag{S94}$$

here u_0 is the scalar part, and J_z is the spin-dependent exchange interaction part of the scattering potential. Solving numerically Eq. S92 up to the potential radius R_0 gives one the values $\vec{A}_m = \vec{A}(r = R_0)$ and allows one to express the elements of K_m and S_m though $\vec{A}_m$, thus restoring the scattering amplitude.

C. Numerical results

Below we focus on a nonmagnetic spectrum ($h = 0$) and present the calculated scattering cross-section for the Rashba electrons on a magnetic impurity described by the model potential

$$V(r) = u_0(r) + u_{ex}(r)\hat{\sigma}_z. \tag{S95}$$

To describe the skew scattering we introduce symmetric and asymmetric combinations of the scattering cross-section

$$\sigma_{ij}^{s,a}(\theta) = \frac{1}{2}\left(\sigma_{ij}(\theta) \pm \sigma_{ij}(-\theta)\right). \tag{S96}$$

For a purely scalar potential $u_{ex} = 0$ the calculated asymmetric part $\sigma_{ij}^{a}(\theta) = 0$ is always zero, in full agreement with the fact, that for the Rashba ferromagnetic model it appears only in view of nonzero Zeeman splitting h. For nonmagnetic electrons the skew scattering can be induced due to impurity finite magnetic moment, as analyzed analytically in the main text.

In Fig. S2 we present the calculated differential cross-sections in different scattering channels for a short range potential of radius $R_0 \ll k_{1,2}^{-1}$. The profile of the functions $u(r), u_{ex}(r)$ is taken constant for $r < R_0$. A series of figures in Fig. S2 correspond to different relative magnitudes of u_{ex}/u_0. The increase of the skew scattering is clearly associated with the increase in the magnitude of the exchange interaction part.

[S1] M. A. Rakitskii, K. S. Denisov, I. V. Rozhansky, and N. S. Averkiev, Fingerprints of the electron skew scattering on paramagnetic impurities in semiconductor systems, Applied Physics Letters **118**, 032105 (2021).
[S2] E. Ivchenko, *Optical Spectroscopy of Semiconductor Nanostructures* (Alpha Science International, Harrow, UK, 2005).